Prospects and Possibilities for Connecting Ductile Fracture Toughness and the Statistics of Fracture Surface Roughness

Alan Needleman
Department of Materials Science & Engineering
University of North Texas

Work with:

Ankit Srivastava, Shmulik Osovski, Laurent Ponson, Viggo Tvergaard, Elisabeth Bouchaud, James C. Williams

UNT
UNIVERSITY OF NORTH TEXAS

Materials Fracture Mechanics

- Fundamental issues:
  - What is the relation between crack growth resistance, microstructure and applied loading?
  - What is the relation between fracture surface roughness, microstructure and applied loading?
    - Corollary: What is the relation, if any, between a material system's crack growth resistance and the statistics of fracture surface roughness?
- Aim: simulate ductile fracture for model microstructures and predict the crack growth resistance and the fracture surface roughness.
  - Can the analyses be used to develop a design methodology for materials with improved failure resistance?

UNT
UNIVERSITY OF NORTH TEXAS

Toughness/Roughness Relation

- Possible uses:
  - Provide a quantitative measure of toughness (crack initiation and growth resistance) in circumstances where a valid fracture test cannot be carried out.
  - Identify and provide insight into the physical mechanism of crack initiation/growth.
  - Provide a basis for assessing the predictive capability of theories of crack initiation and growth.

UNT
UNIVERSITY OF NORTH TEXAS

Ductile Fracture in Structural Metals

- Ductile fracture limits the performance, reliability and manufacturability of a variety of engineering components and structures.

www.seattlerobotics.org

http://www.ntsb.gov

www.geekologie.com

UNT
UNIVERSITY OF NORTH TEXAS

Ductile Fracture in Structural Metals

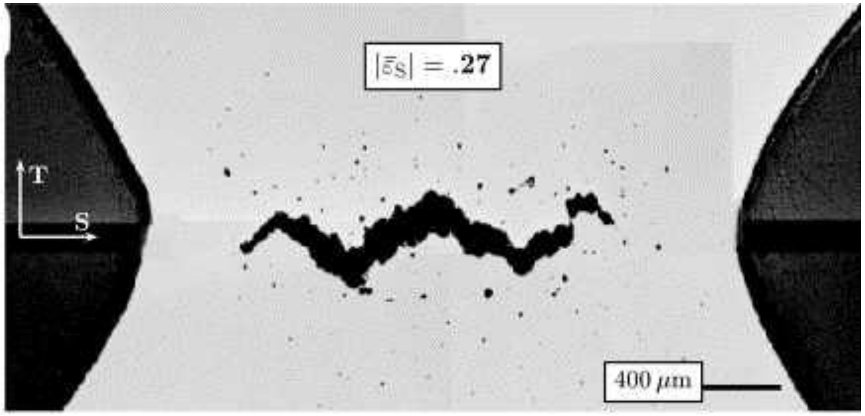

Benzerga et al. (2004)

- Near room temperature the main mechanism of ductile failure in structural metals involves the nucleation, growth and coalescence of voids originating at second phase particles.
  - The key role played by porosity in ductile fracture was identified Tipper (1949).
  - Puttick (1959), Rogers (1960), Beachem (1963) and Gurland and Plateau (1963) documented the process of micro-void evolution.

UNIVERSITY OF NORTH TEXAS

Void Nucleation, Growth and Coalescence

- Void nucleation by inclusion debonding or cracking.
- Void growth occurs by plastic deformation of the matrix.
- Void coalescence occurs either by impingement or through a void sheet.

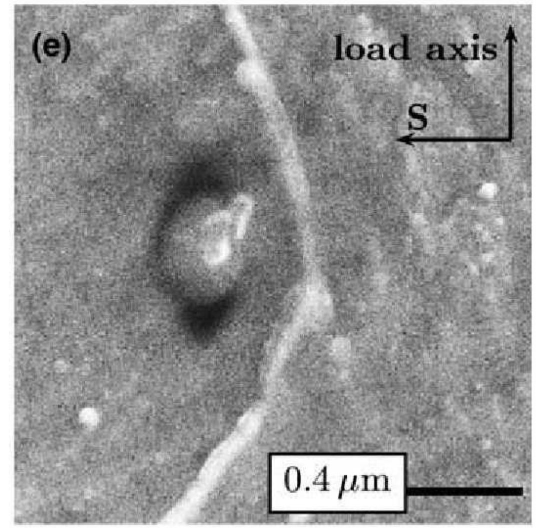

Benzerga et al. (2004)

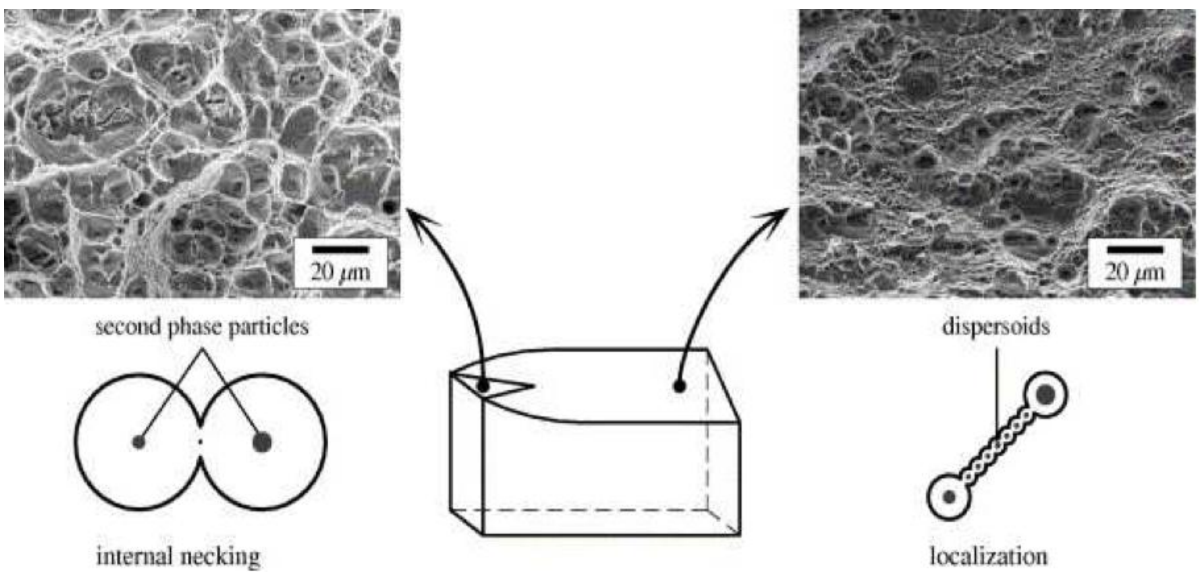

Bron and Besson (2006)

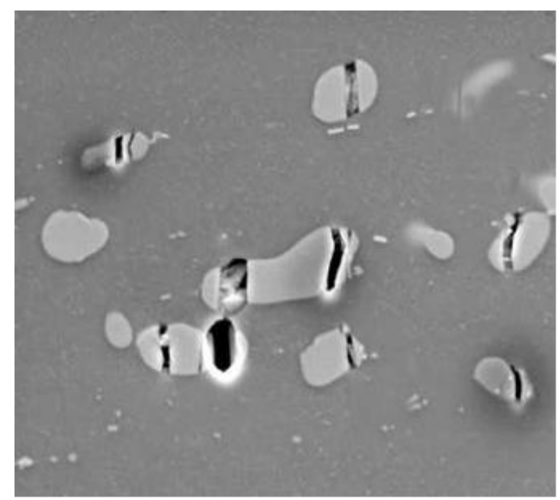

Brocks (2008)

UNIVERSITY OF NORTH TEXAS

Ductile Crack Growth

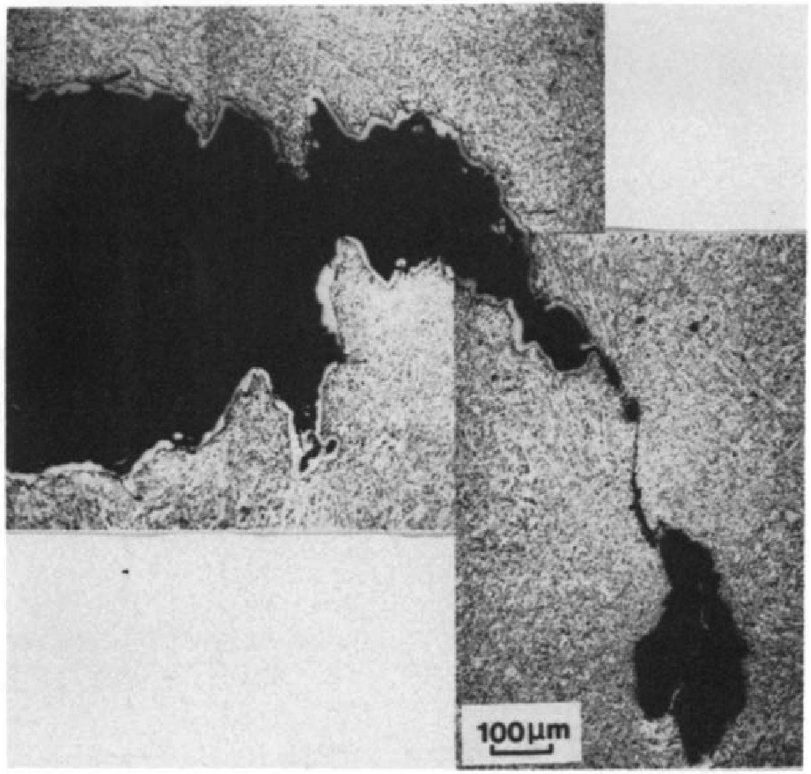

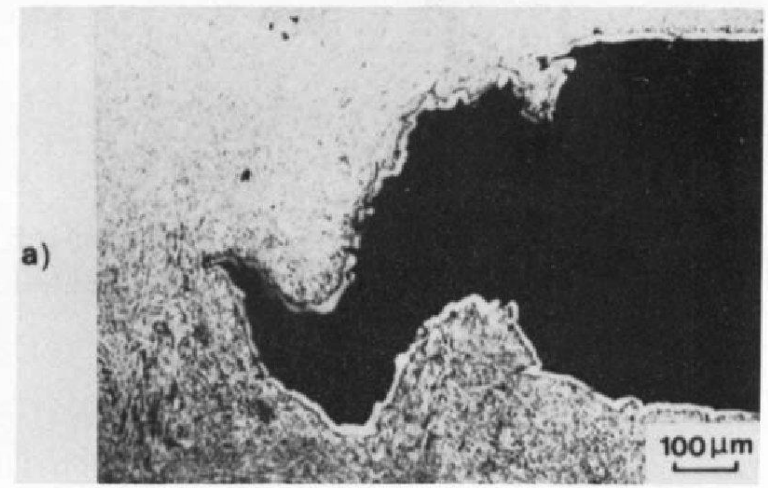

- Atomic work of separation: 1-10 J/m^2.
- Work per unit area of crack advance for ductile metals: 10^4-10^5 J/m^2.

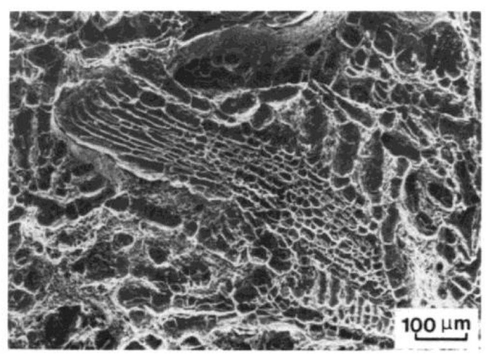

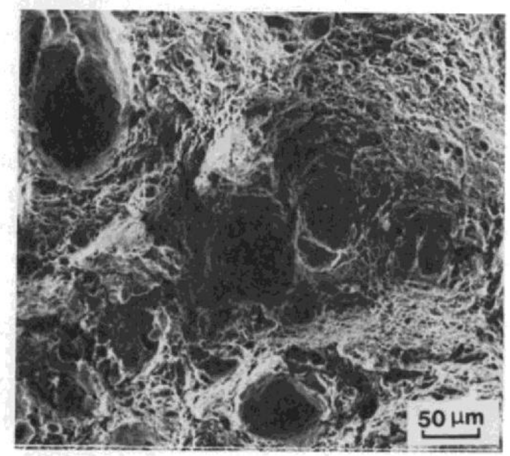

Lautridou and Pineau,
Eng. Fract. Mech., 15, 55, 1981

UNT
UNIVERSITY OF NORTH TEXAS

Modified Gurson Relation

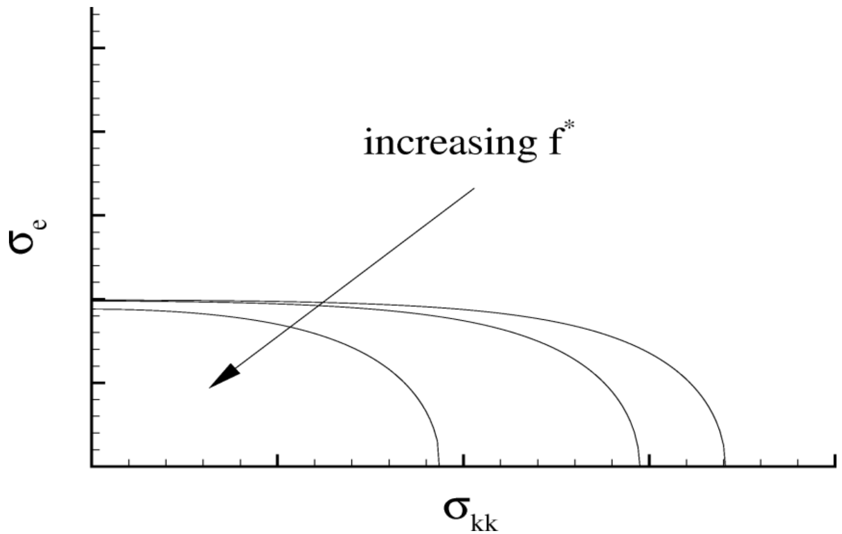

$$\dot{f} = (1-f)\mathbf{d}^p : \mathbf{I} + \dot{f}_{nucl}$$

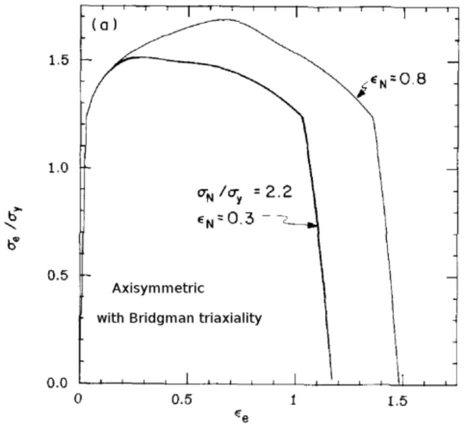

$$\Phi(\sigma_{ij}, \bar{\sigma}, f) = \frac{\sigma_e^2}{\bar{\sigma}^2} + 2q_1 f^* \cosh\left(\frac{q_2\sigma_{kk}}{2\bar{\sigma}}\right) - 1 - (q_1 f^*)^2 = 0$$

$$f^* = \begin{cases} f & f < f_c \\ f_c + (1/q_1 - f_c)(f - f_c)/(f_f - f_c) & f \geq f_c \end{cases}$$

Matrix flow strength $\bar{\sigma}$ Void volume fraction *f*

- The stress carry capacity vanishes when $f^*=1/q_1$ which is when $f=f_f$ (the surface $\Phi= 0$ shrinks to a point) and new free surface is created.

UNIVERSITY OF NORTH TEXAS

Rice & Tracey (1969); Gurson (1975); Tvergaard (1981, 1982); Tvergaard & Needleman (1984)

Heterogeneous Material Microstructures Analyzed

- Random 3D array of discretely modeled void nucleation sites (“inclusions”)
    - Length scale: mean nucleation site spacing.
- Grain boundary fracture in a 2D polycrystal
    - Length scale: mean grain size.

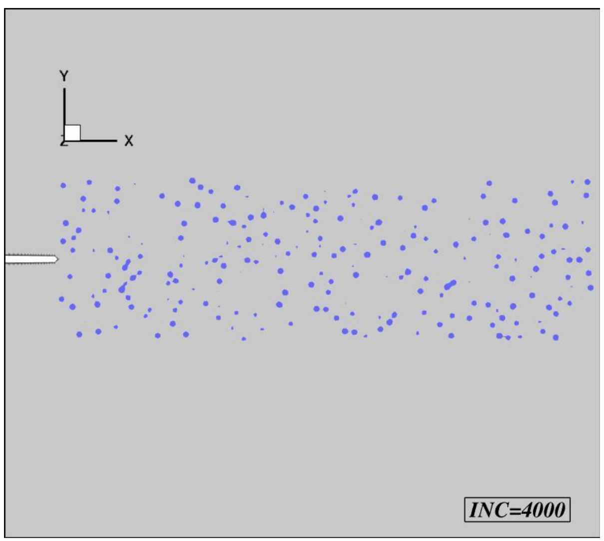

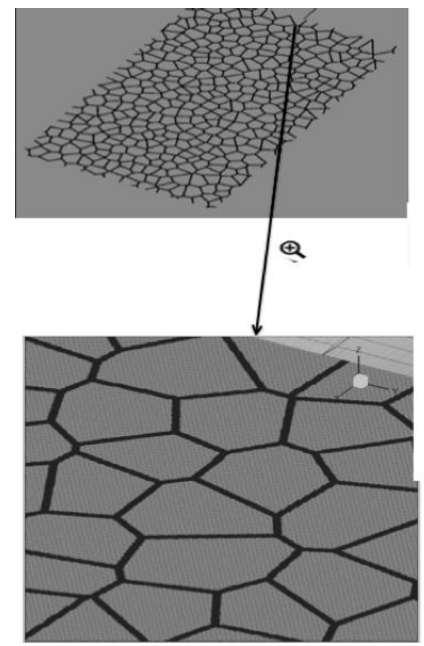

UNT
UNIVERSITY OF NORTH TEXAS

Void Nucleation

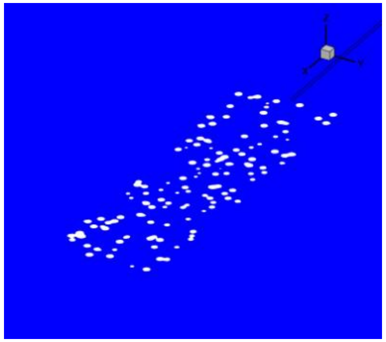

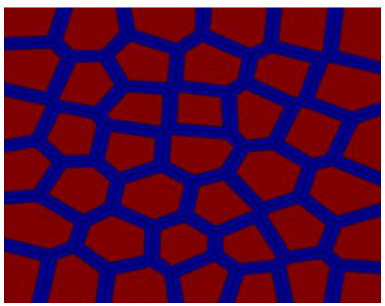

- Large, low strength regions that are modeled by stress controlled nucleation.

$$\dot{f}_{nucl}^{\text{stress}} = A\left[\dot{\bar{\sigma}} + \dot{\sigma}_h\right]\ ,\ A = \frac{f_N^{\text{stress}}}{s_N^{\text{stress}}\sqrt{2\pi}} \exp\left[-\frac{1}{2}\left(\frac{\bar{\sigma} + \sigma_h - \sigma_N}{s_N^{\text{stress}}}\right)^2\right]$$

- Spherical inclusions (3D "islands" of f_N) with randomly distributed centers or within grain boundary layers of a prescribed thickness.

$$f_N^{\text{stress}} = \begin{cases} \bar{f}_N^{\text{stress}} & \text{in specified region} \\ 0 & \text{otherwise} \end{cases}$$

- Uniformly distributed sites (small particles) that are modeled by strain controlled nucleation (no characteristic length).

$$\dot{f}_{nucl}^{\text{strain}} = D\dot{\bar{\epsilon}}\ ,\ D = \frac{f_N^{\text{strain}}}{s_N^{\text{strain}}\sqrt{2\pi}} \exp\left[-\frac{1}{2}\left(\frac{\bar{\epsilon} - \epsilon_N}{s_N^{\text{strain}}}\right)^2\right]$$

$$f(0) = 0$$

UNT
UNIVERSITY OF NORTH TEXAS

Small-Scale Yielding Boundary Value Problem

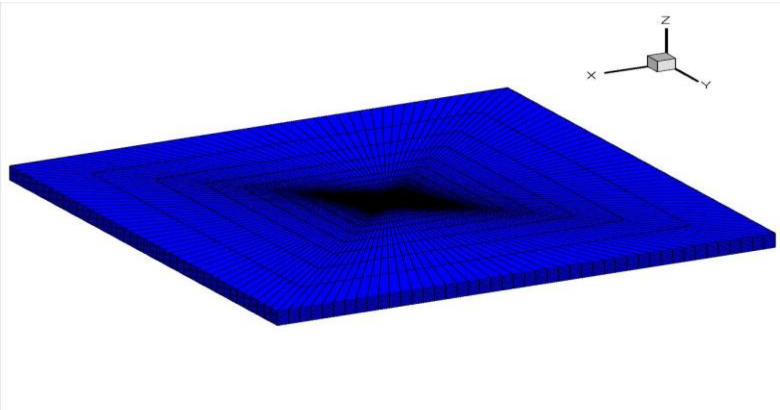

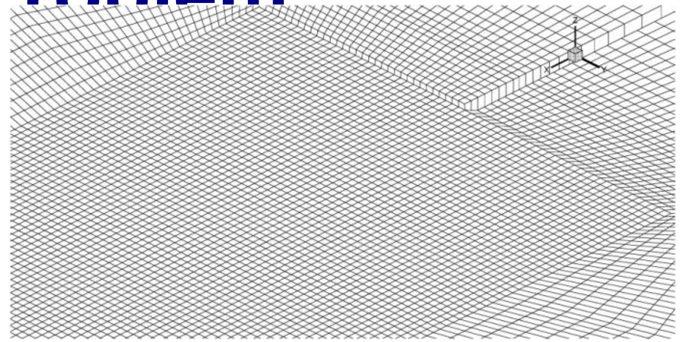

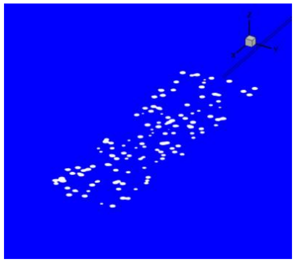

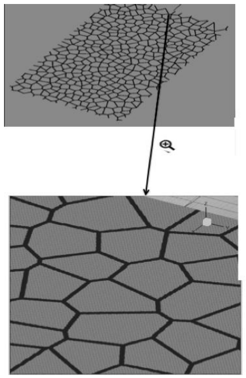

$K_I(t)$ applied

- **A thin strip** subject to overall plane strain conditions.
- 3D dynamic finite strain formulation.

$$\int_V \tau^{ij}\delta E_{ij}\,dV = \int_S T^i \delta u_i\,dS - \int_V \rho \frac{\partial u^i}{\partial t}\delta u_i\,dV$$

- Displacements corresponding to the isotropic elastic mode I field are imposed on the remote boundaries.
- Initial and boundary conditions chosen to minimize wave effects.

UNT
UNIVERSITY OF NORTH TEXAS

Possible Length Scales

- **Macro length scale J/σ_0**
- **The mean inclusion spacing.**
- **The grain size.**
- The inclusion size.
- The grain boundary layer thickness.
- Material rate dependence also provides regularization and thus implicitly introduces a length.
- **The finite element mesh length scale.**
  - Can dominate in the limit of a homogeneous material - no inclusions or all inclusions, and no grains.

$$J = K_I^2 \frac{(1-\nu^2)}{E}$$

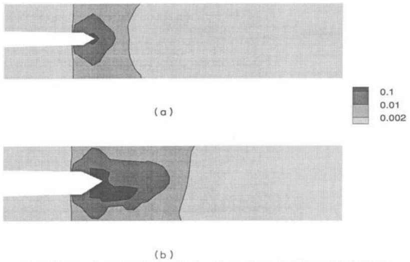

Fig. 10. Contours of constant void volume fraction, f, for a uniform material (no inclusions) using the mesh in Fig. 3a. (a) $t = 1.30\ \mu$sec; (b) $t = 1.74\ \mu$sec.

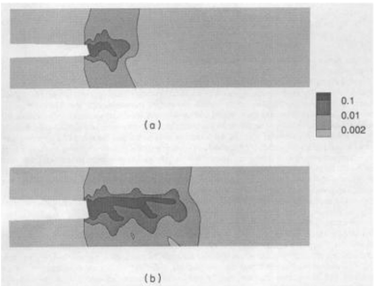

Fig. 12. Contours of constant void volume fraction, f, for a uniform material (no inclusions) using the mesh in Fig. 3c. (a) $t = 1.16\ \mu$sec; (b) $t = 1.38\ \mu$sec.

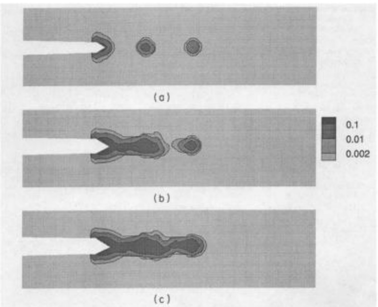

Fig. 7. Contours of constant void volume fraction, f, for the initially sharp crack tip configuration in Fig. 5a and using the mesh in Fig. 3b. (a) $t = 1.20\ \mu$sec; (b) $t = 1.30\ \mu$sec; (c) $t = 1.33\ \mu$sec.

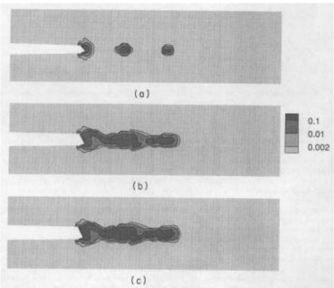

Fig. 8. Contours of constant void volume fraction, f, for the initially sharp crack tip configuration in Fig. 5a and using the mesh in Fig. 3c. (a) $t = 1.10\ \mu$sec; (b) $t = 1.20\ \mu$sec; (c) $t = 1.21\ \mu$sec.

UNT
UNIVERSITY OF NORTH TEXAS

Needleman and Tvergaard, Eng. Frac. Mech., 47, 75, 1994.

Microstructure with Discretely Modeled Inclusions

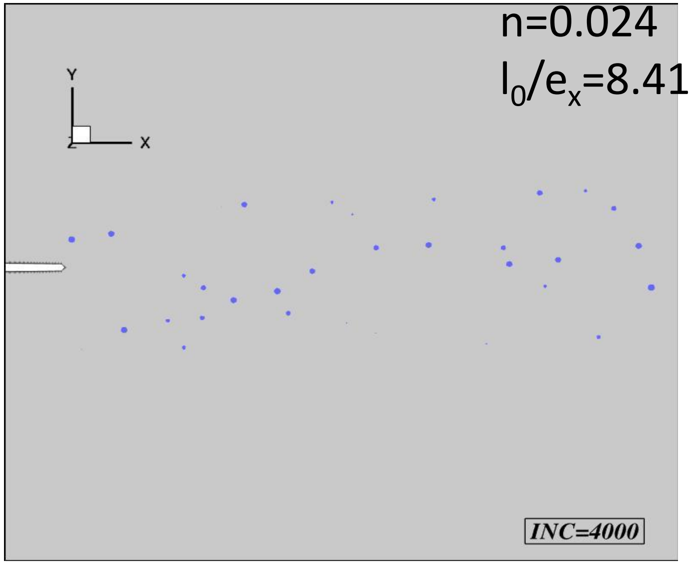

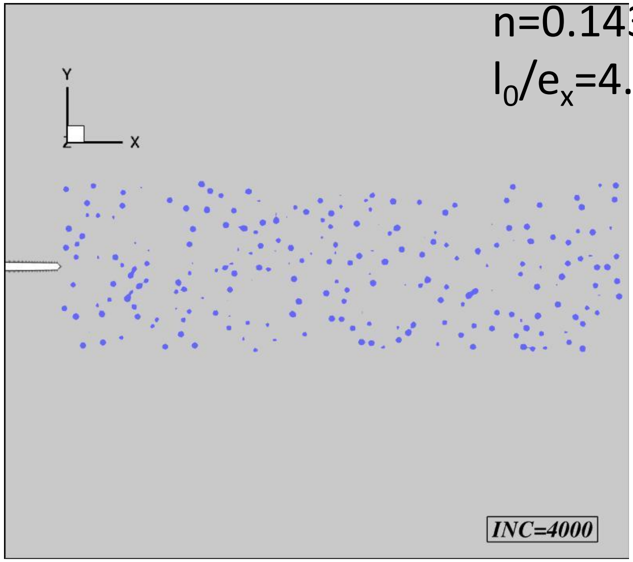

- Calculations carried out for eight inclusion volume fractions/spacings; n=0.012 to n=0.19; l_0=10.6e_x to 4.21e_x.
  - Seven realizations for each inclusion volume fraction *n*.
  - For the smallest volume fraction results only obtained for five realizations: in two realizations no inclusion sufficiently close to the initial crack tip for small scale yielding crack growth to occur.
  - Fracture surface is f=0.1 (the material has essentially lost all stress carrying capacity).

UNT UNIVERSITY OF NORTH TEXAS

Srivastava et al., J. Mech. Phys. Solids, 63, 62-79, 2014.
Osovski et al., The effect of loading rate on ductile fracture toughness and fracture surface roughness. J. Mech. Phys. Solids, accepted.

Crack Growth – Low Inclusion Density

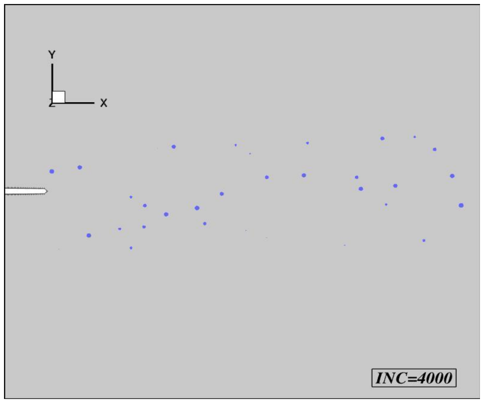

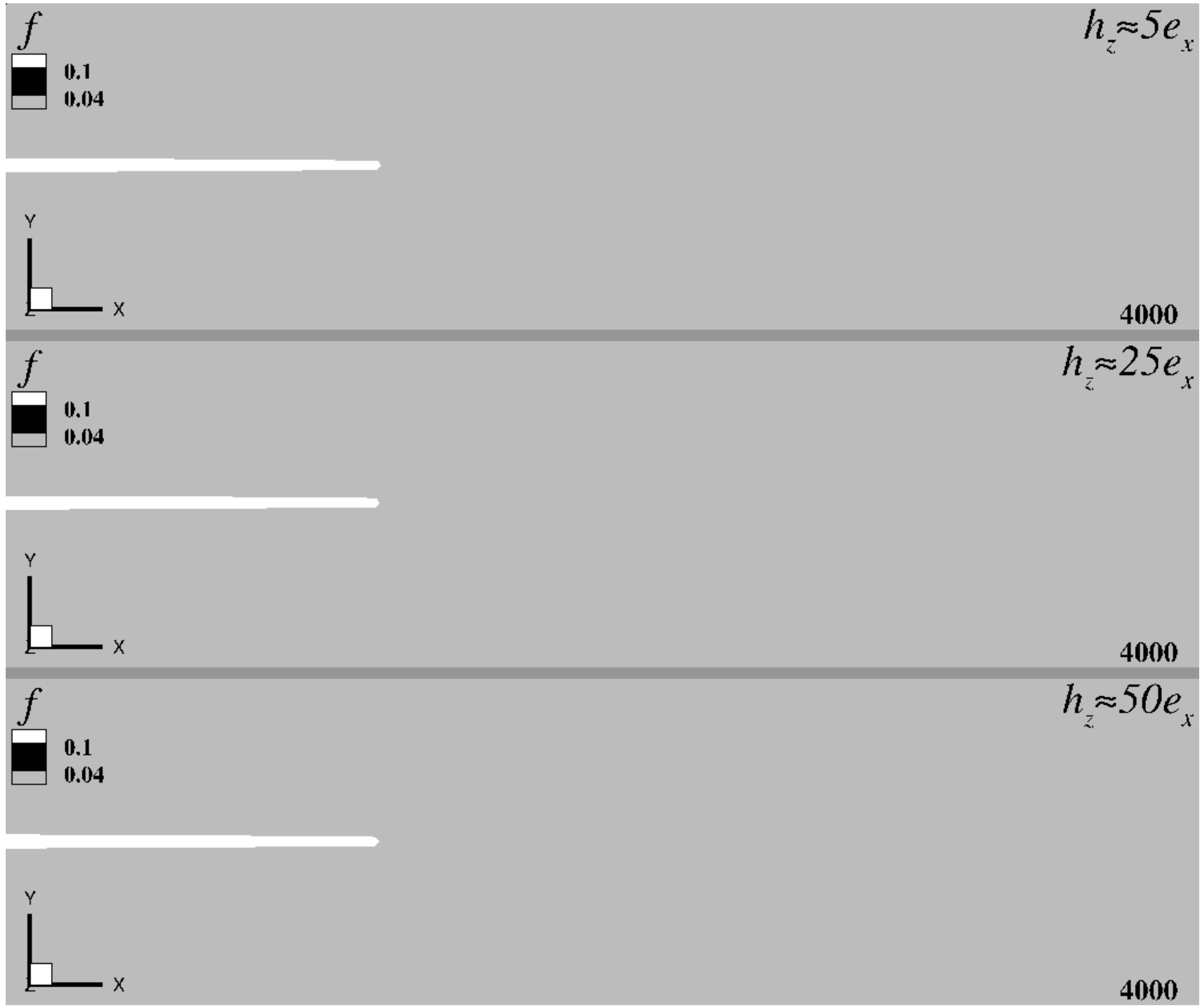

n=0.024
l_0/e_x=8.41

UNIVERSITY OF NORTH TEXAS

Three through thickness slices.

Crack Growth – High Inclusion Density

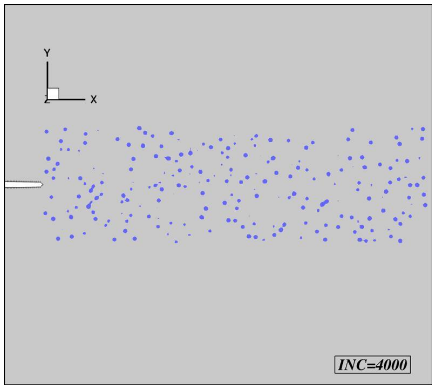

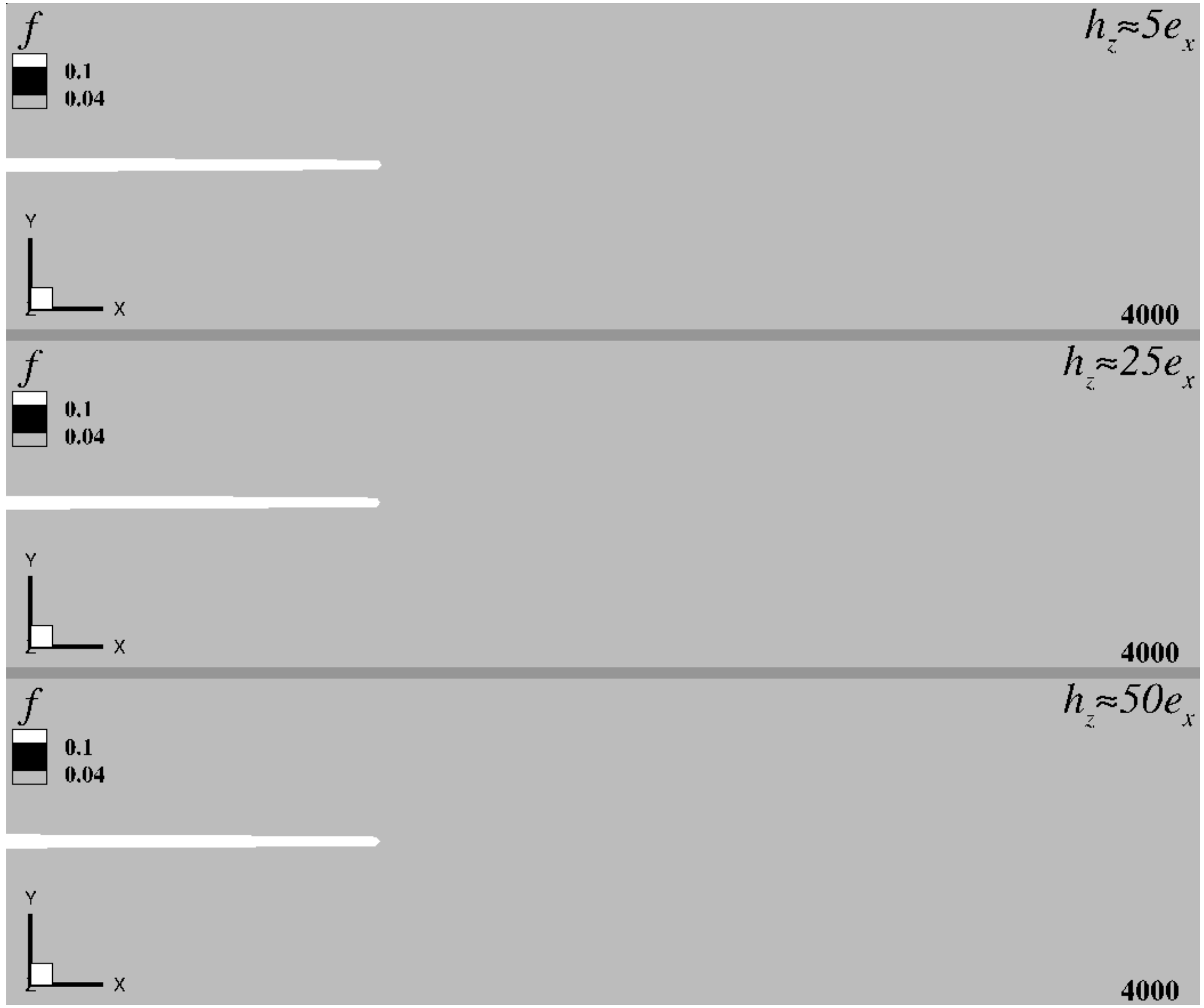

$n=0.143$
$l_0/e_x=4.63$

Three through thickness slices.

UNT UNIVERSITY OF NORTH TEXAS

Void-Crack Interaction Near a Crack Tip

V. Tvergaard, J.W. Hutchinson / International Journal of Solids and Structures 39 (2002) 3581–3597

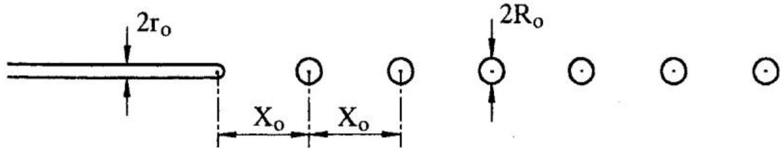

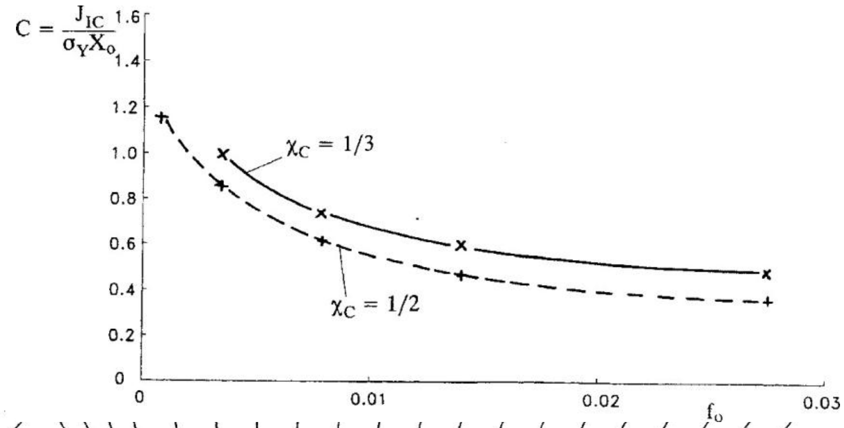

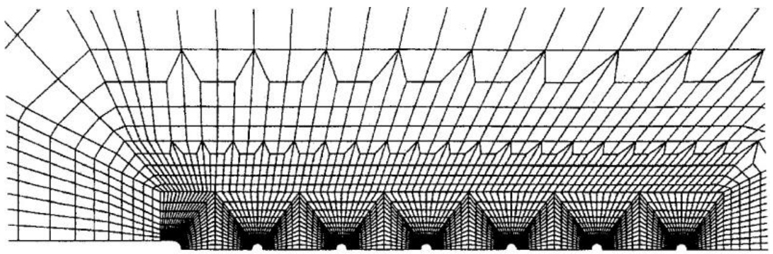

(a)

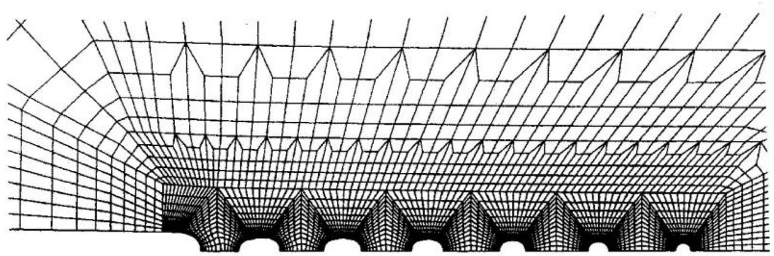

(b)

High volume fraction – multiple voids interaction crack growth

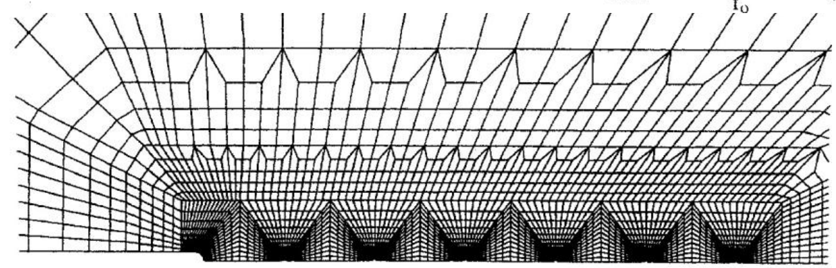

(a)

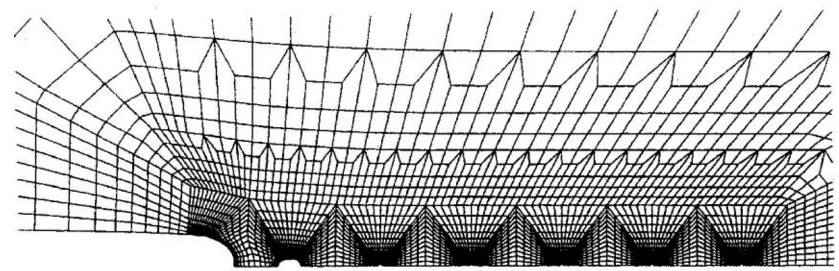

(b)

Low volume fraction – void by void crack growth

UNIVERSITY OF NORTH TEXAS

J-R Curves – Variation with Inclusion Density

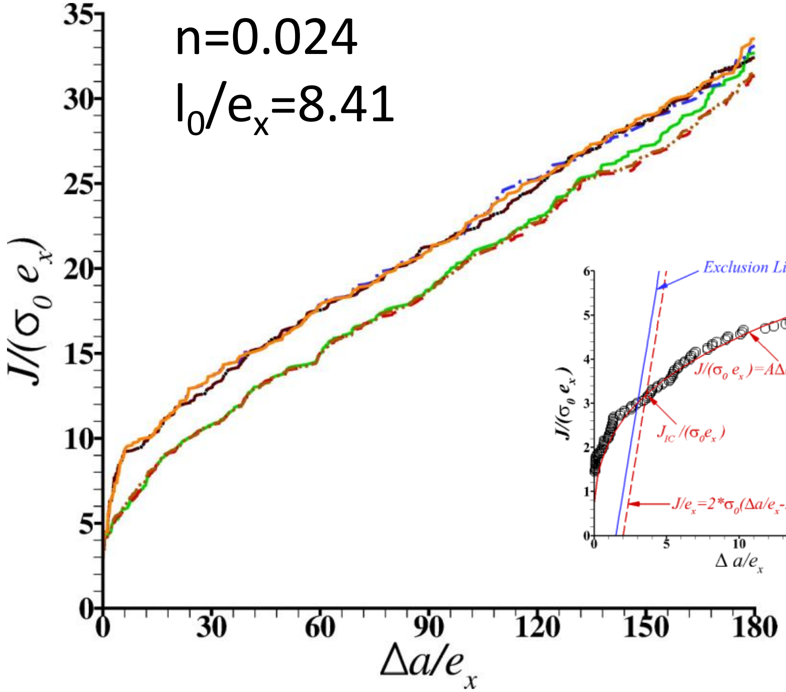

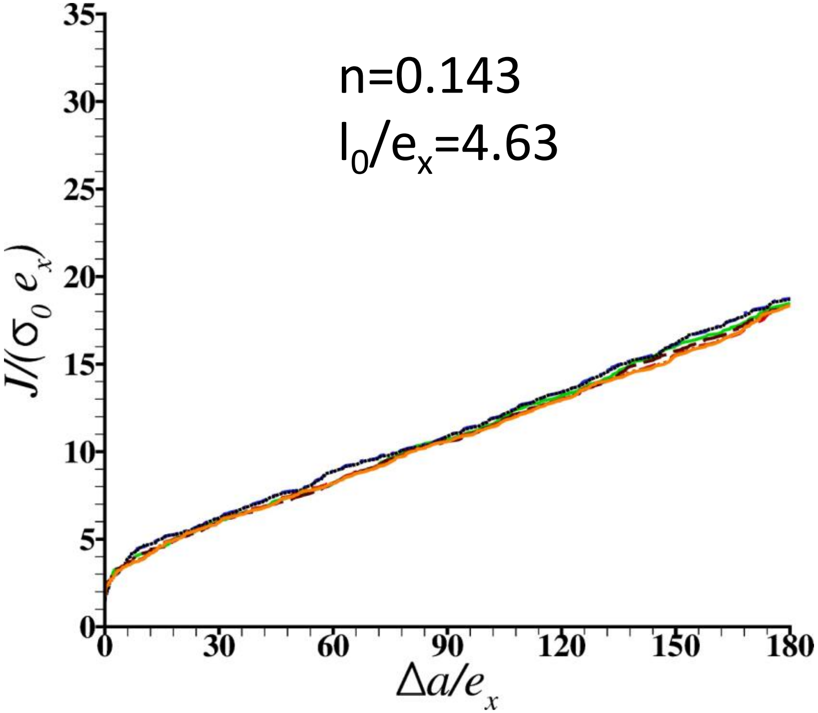

- Compute J-R where curves (Δa is defined by the extent of the f=0.10 contour).
  - e_x is the mesh spacing (a fixed reference length).
- Compute J_{IC} mimicking the ASTM E1820-11 standard procedure.
- T_R is computed from the slope between $\Delta a/e_x$=100 and 150.

UNIVERSITY OF NORTH TEXAS

Variation of J_{IC} and T_R with Inclusion Spacing

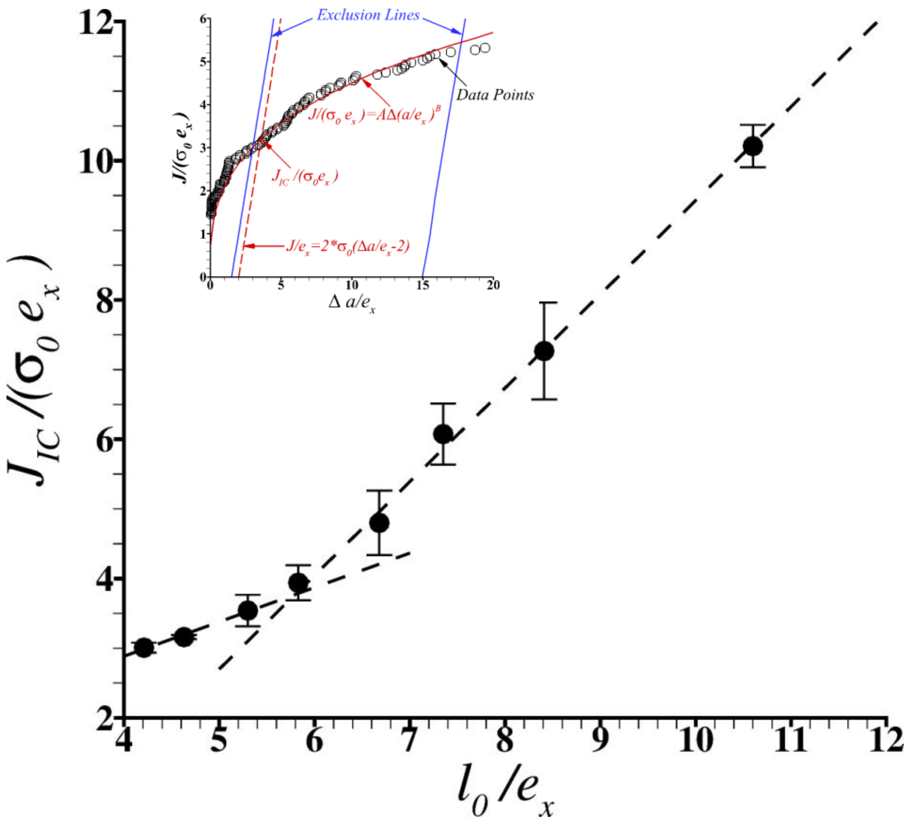

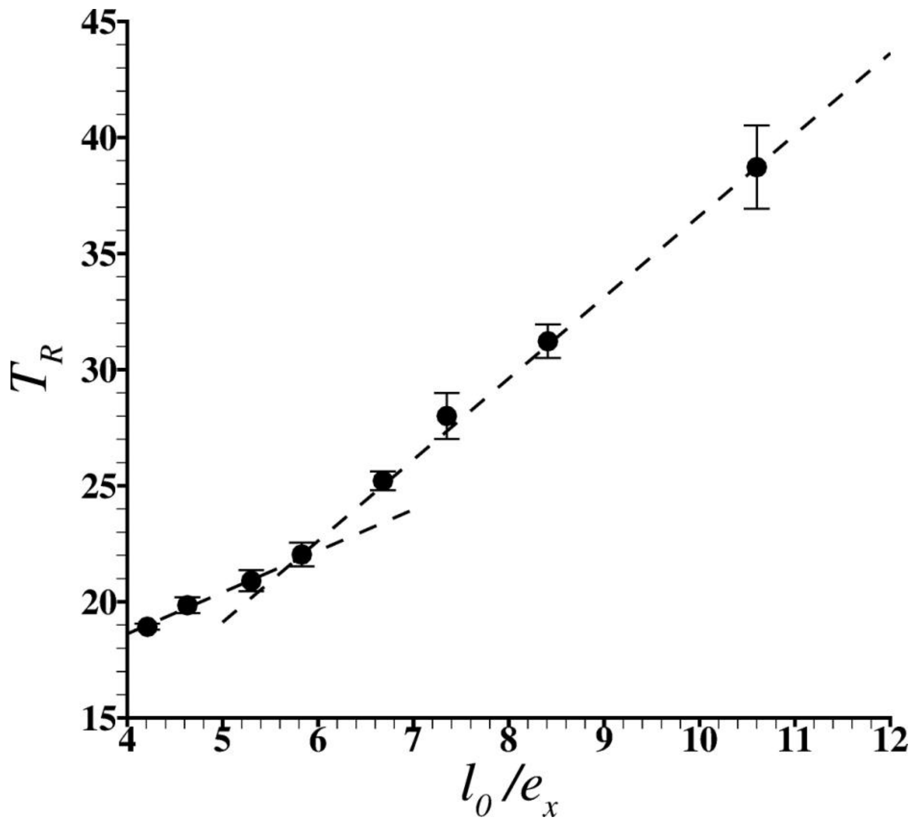

- Compute J_{IC} mimicking the ASTM E1820-11 standard procedure.
- T_R is computed from the slope between $\Delta a/e_x$=100 and 150.
- l_0 is the mean inclusion spacing.

$$J_{IC} = K_{IC}^2 \frac{(1-\nu^2)}{E} \qquad T_R = \left(\frac{E}{\sigma_0^2}\right)\frac{dJ}{d(\Delta a)}$$

UNT UNIVERSITY OF NORTH TEXAS

J-R curves – Variation with Loading Rate

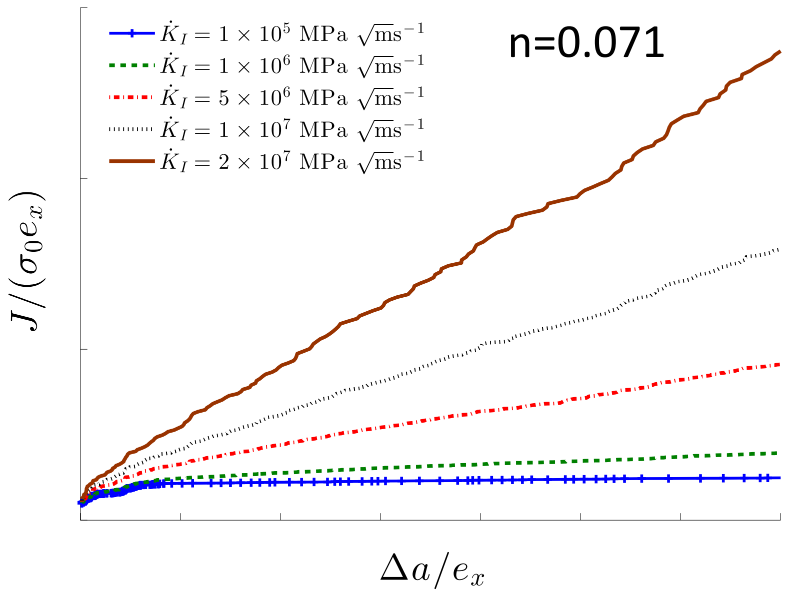

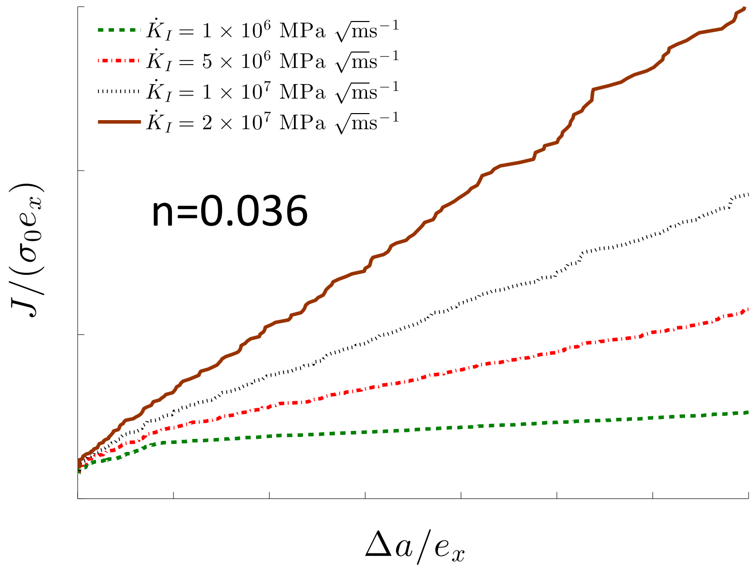

- Only one realization for each loading rate.
- The crack growth resistance increases with increasing loading rate.
- **A fixed mechanism of void nucleation, growth and coalescence**

UNIVERSITY OF NORTH TEXAS

Effect of Loading Rate on the Ductile Fracture Mode

$$\dot{K}_I = 1 \times 10^5 \mathrm{MPa}\sqrt{\mathrm{m}}s^{-1}$$

$$\dot{K}_I = 5 \times 10^6 \mathrm{MPa}\sqrt{\mathrm{m}}s^{-1}$$

$$\dot{K}_I = 5 \times 10^7 \mathrm{MPa}\sqrt{\mathrm{m}}s^{-1}$$

n=0.071

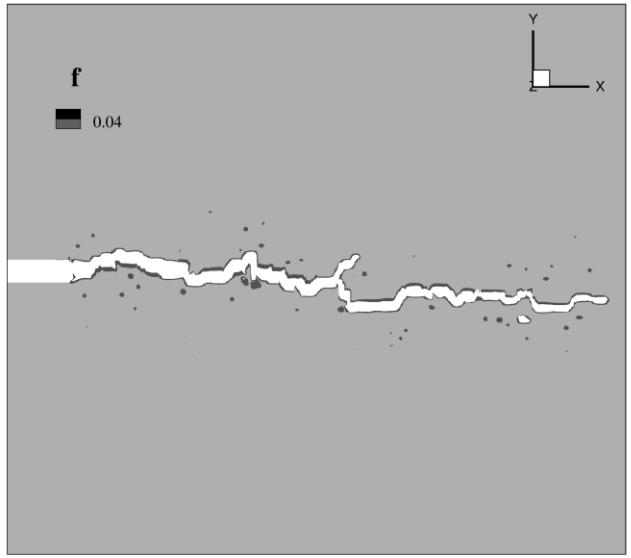

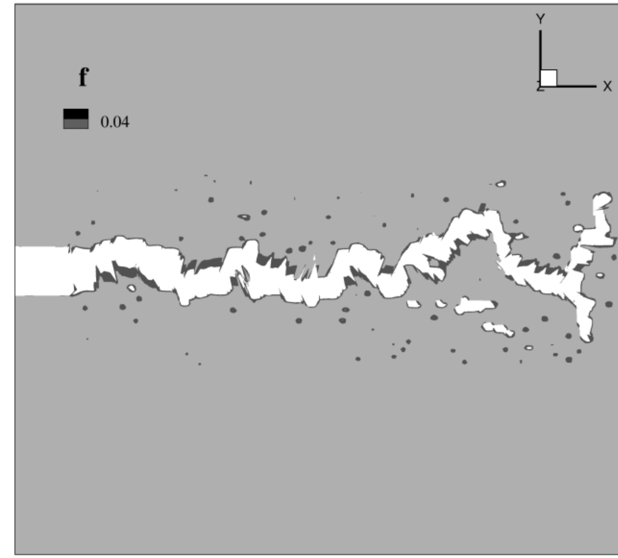

Void-by-void dominated.

Multiple void interaction dominated.

Nucleation dominated distributed damage.

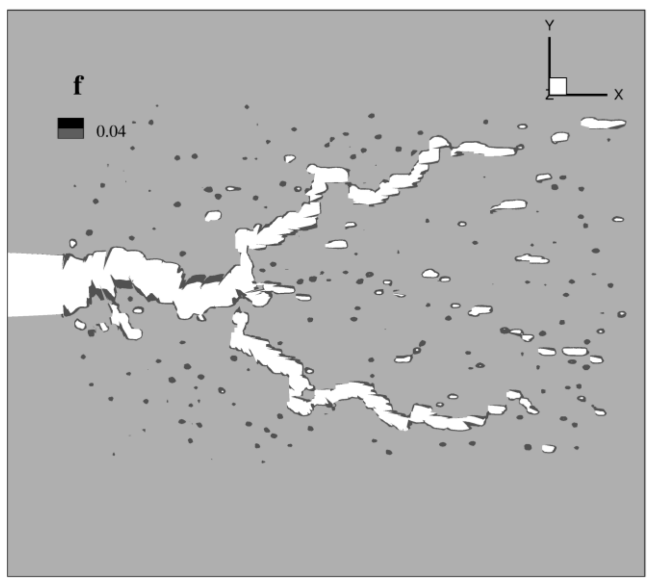

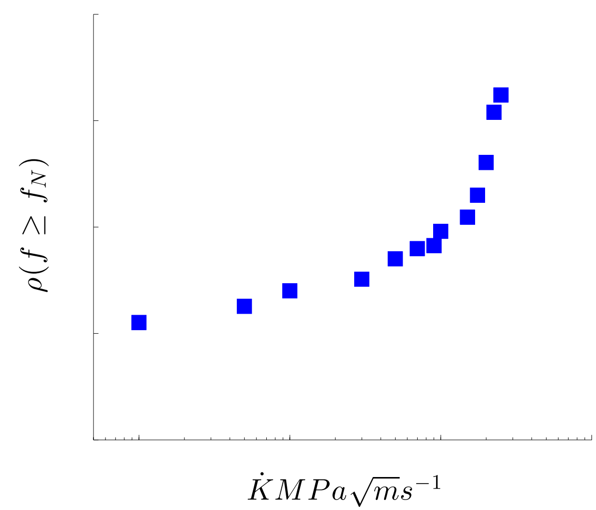

Variation of Plastic Dissipation with Loading Rate

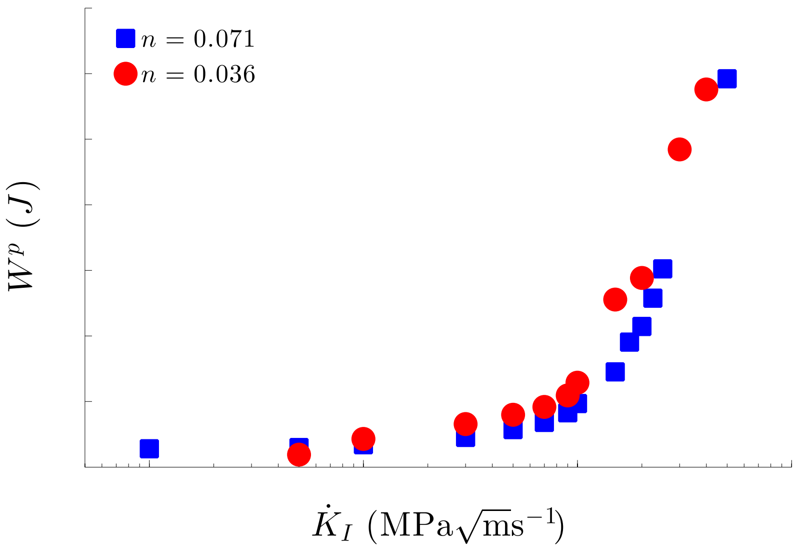

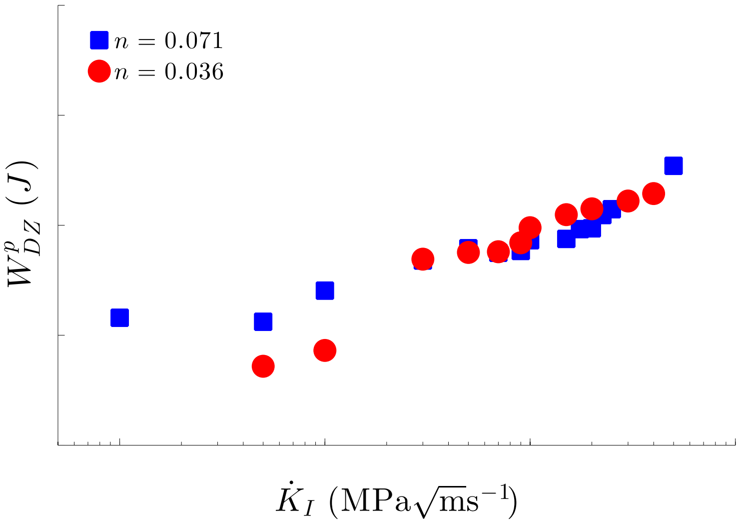

$$W^p(t) = \int_0^t \left[\int \tau : \mathbf{d}^p dV \right] dt$$

$$W^p_{DZ} = \int_0^t \left[\int \tau : \mathbf{d}^p dV_{(f \geq f_N)} \right] dt$$

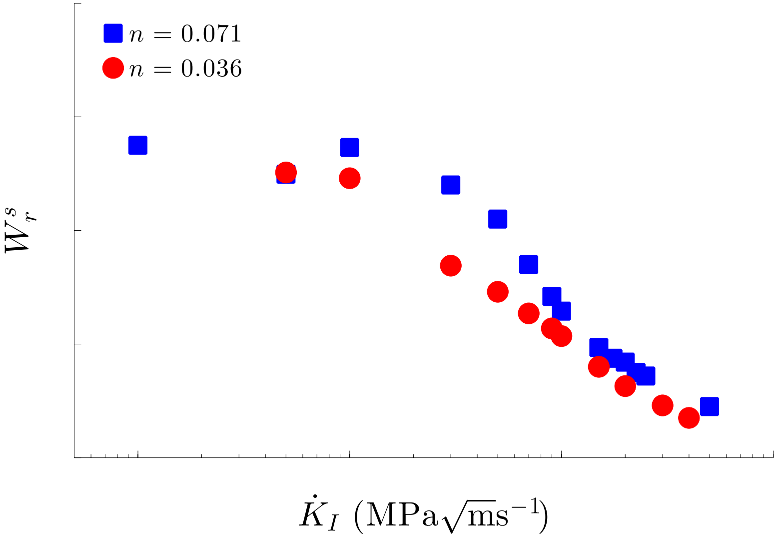

UNT
UNIVERSITY OF NORTH TEXAS

Calculation of the Fracture Surface Roughness

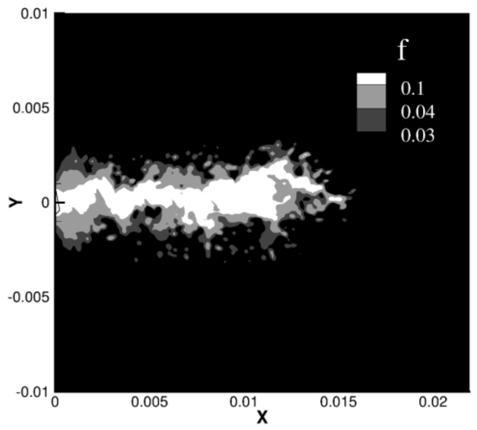

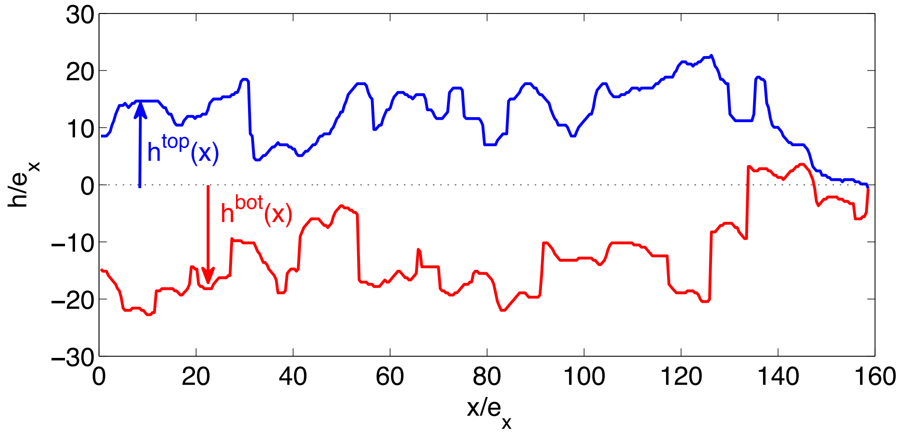

- Thin strip: only roughness in the crack growth direction.
- Mimic the procedure used in the experimental work of Bouchaud, Ponson and co-workers.
    - The fracture surface is identified with a constant value of f.
    - **Extrapolate f to a uniform grid in the fracture plane.**
    - Take cross sections of the "fracture surface" at various planes through the thickness and plot h(x) which at uniformly spaced values of x.

UNT
UNIVERSITY OF NORTH TEXAS

Fracture Surface Statistics – Hurst Exponent

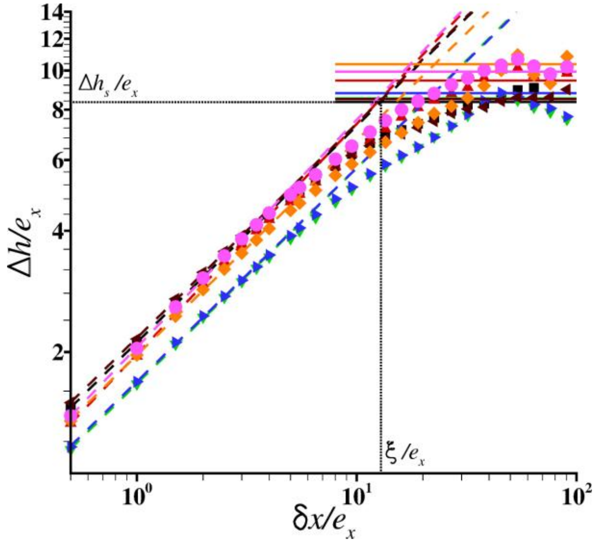

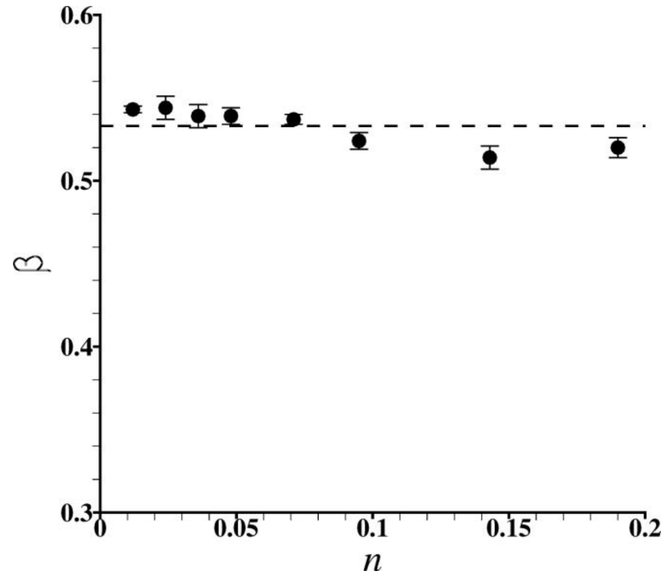

- The small δx Hurst exponent is in the range 0.53 to 0.63.
- The Hurst exponent value depends (within about 0.02) on the extrapolation from finite element Gauss points to a uniform grid.
- The independence of inclusion volume fraction and loading rate does not.

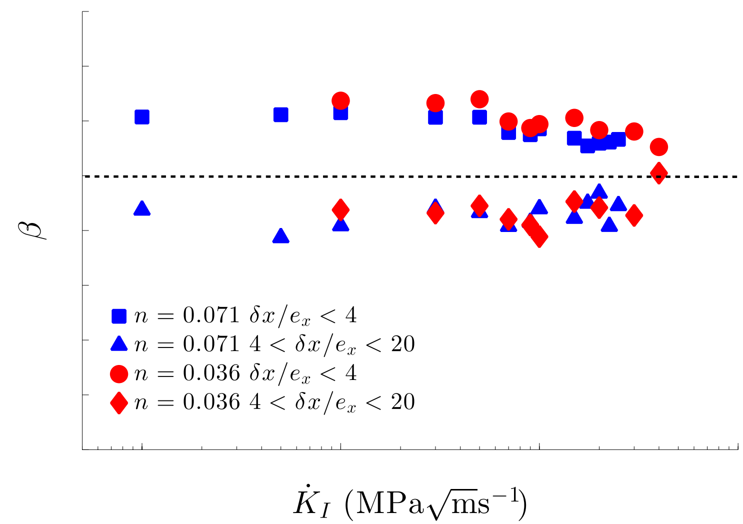

UNIVERSITY OF NORTH TEXAS

$$\Delta h\left(\delta x\right) = \sqrt{\left\langle \left[h\left(x+\delta x, z\right) - h\left(x, z\right)\right]^2 \right\rangle_{x,z}}$$

Fracture Surface Statistics – Beyond the Hurst Exponent

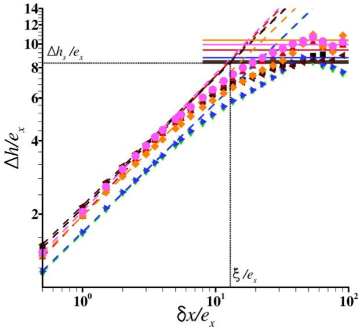

- A transition at about l_0/e_x=6.5 (n=0.07) from void-by-void dominated crack growth to multiple void interaction dominated crack growth.

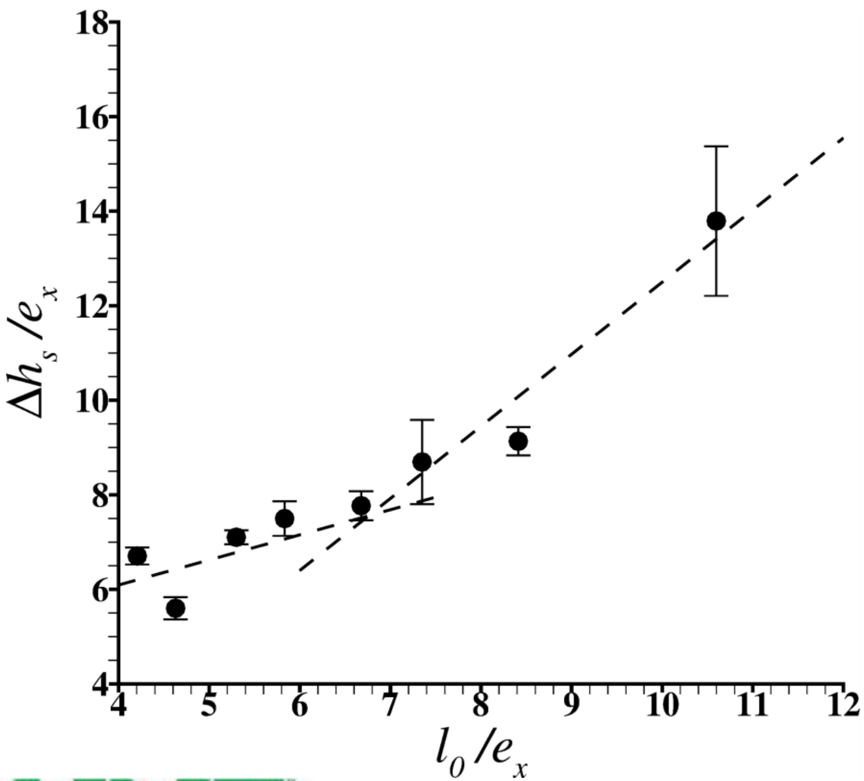

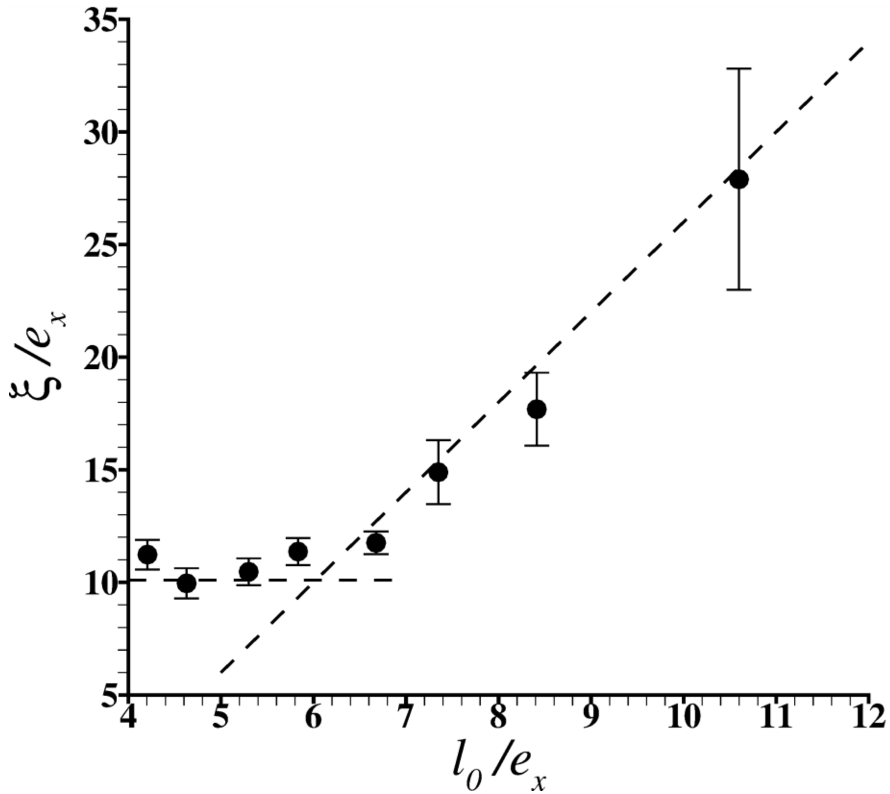

$$\Delta h(\delta x) = \sqrt{\left\langle [h(x+\delta x, z) - h(x,z)]^2 \right\rangle_{x,z}}$$

UNT UNIVERSITY OF NORTH TEXAS

Fracture Surface Statistics – Beyond the Hurst Exponent

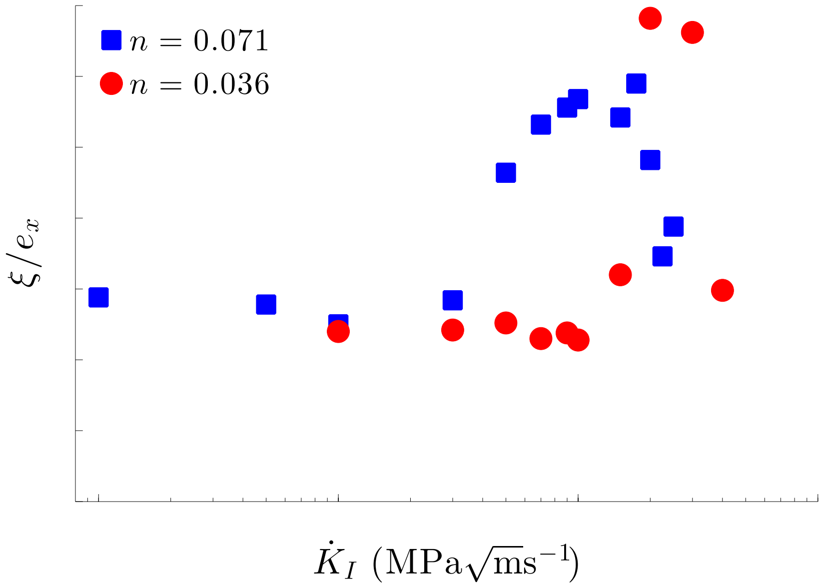

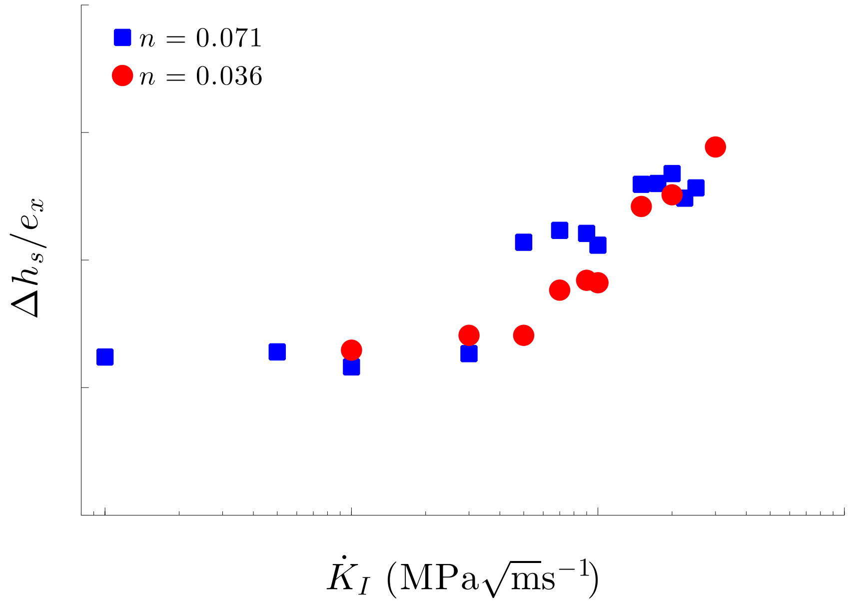

- ξ and Δh_s are nearly independent of loading rate for low loading rates but Δh_s has a more nearly monotonic variation with loading rate for high loading rates, particularly for n=0.036.

UNIVERSITY OF NORTH TEXAS

Fracture Surface Toughness/Roughness Relation

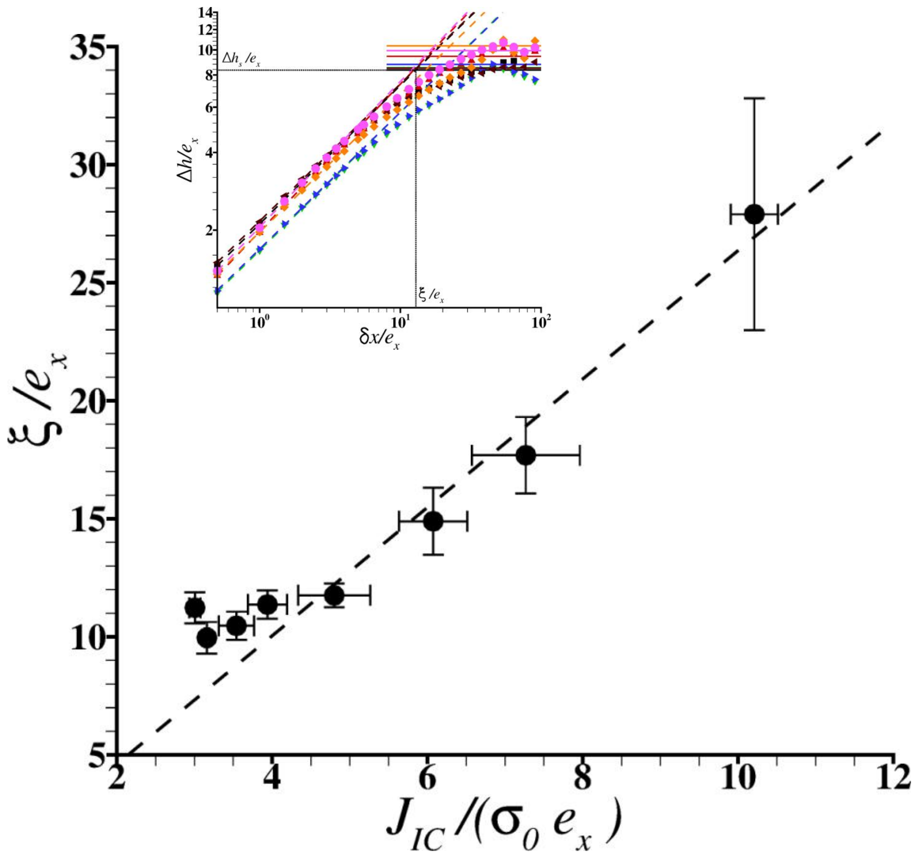

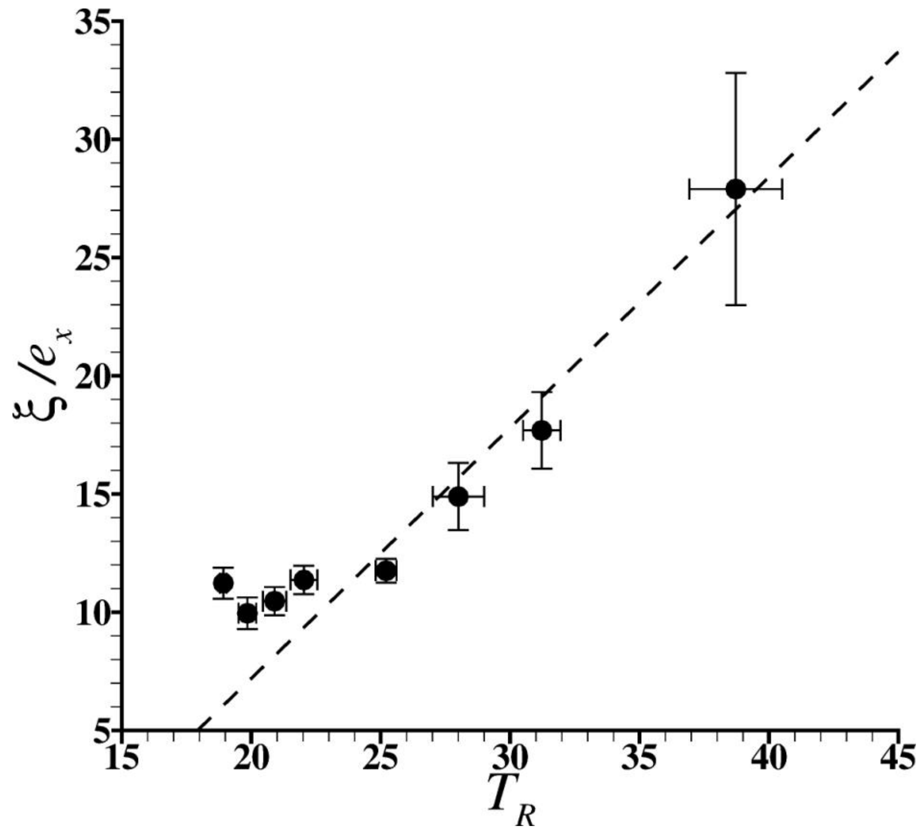

- **Fixed rate; varying inclusion density.**
- Increased surface roughness, increased crack growth resistance.
- Good correlation for roughness values above about 6.5 e_x.

UNIVERSITY OF NORTH TEXAS

Fracture Surface Toughness/Roughness Relation

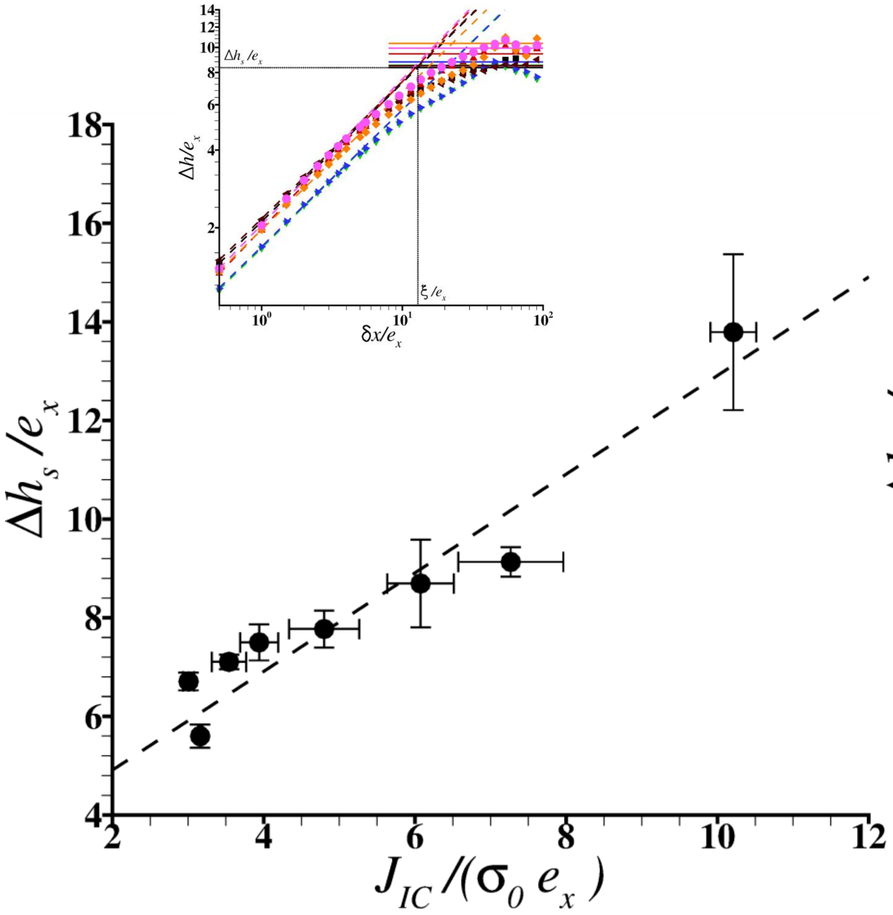

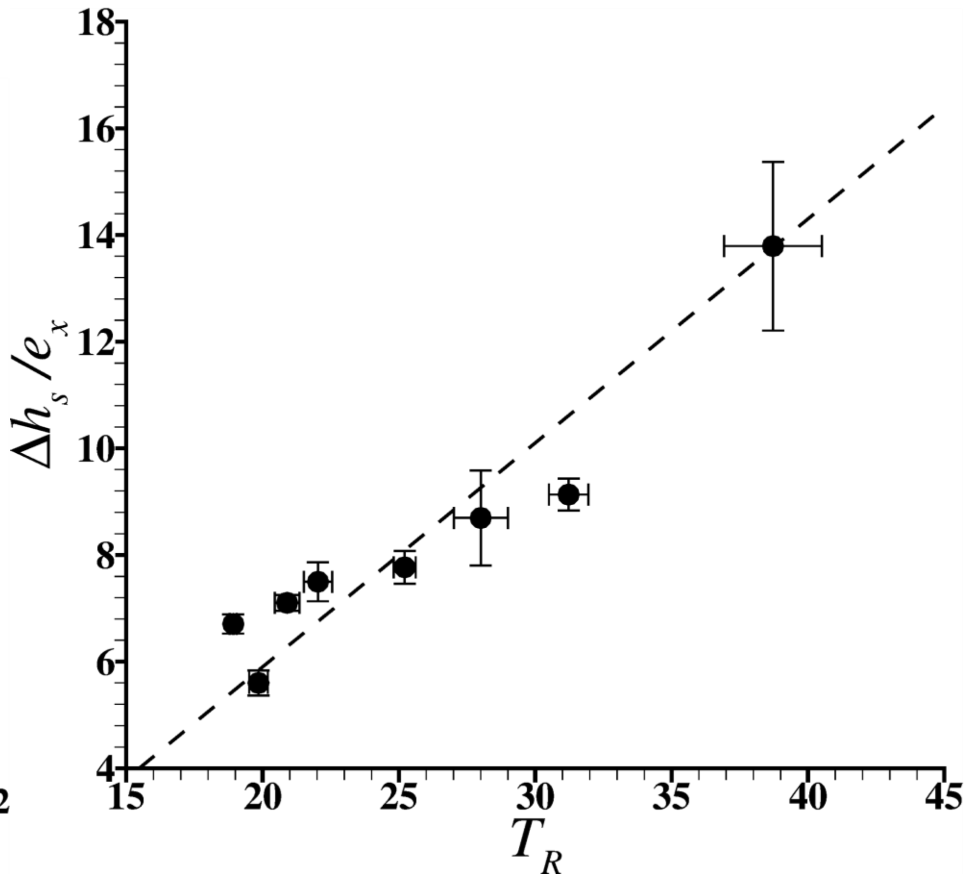

- **Fixed rate; varying inclusion density.**
- Increased surface roughness, increased crack growth resistance.
- Good correlation for roughness values above about 6.5 e_x.

UNIVERSITY OF NORTH TEXAS

Fracture Surface Toughness/Roughness Relation

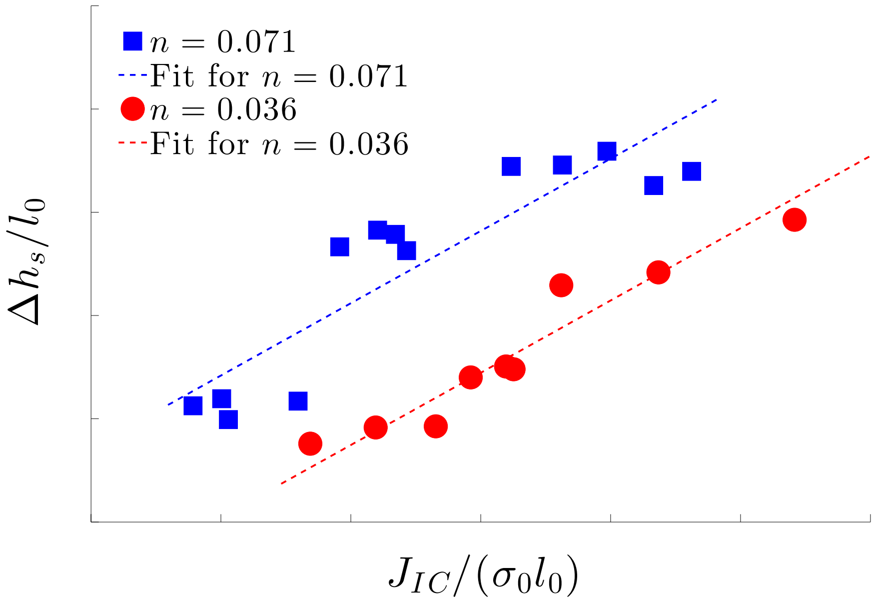

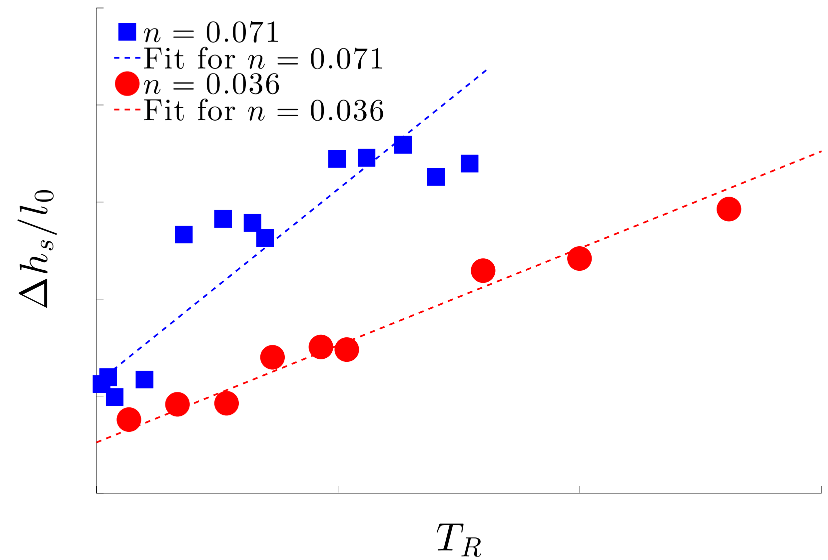

- **Loading rates dK/dt from 1×10^5 to 4×10^7.**
- Inclusion volume fraction n=0.036 corresponds to l_0/e_x=7.35.
  - More void-by-void dominated crack growth.
- Inclusion volume fraction n=0.071 corresponds to l_0/e_x=5.83.
  - Transition from void-by-void to multiple void interaction crack growth.

UNIVERSITY OF NORTH TEXAS

Revisiting the Scaling of the Correlation Function

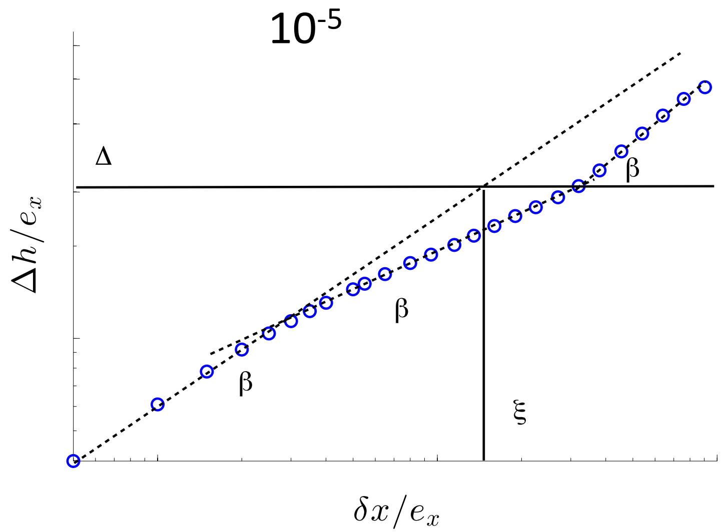

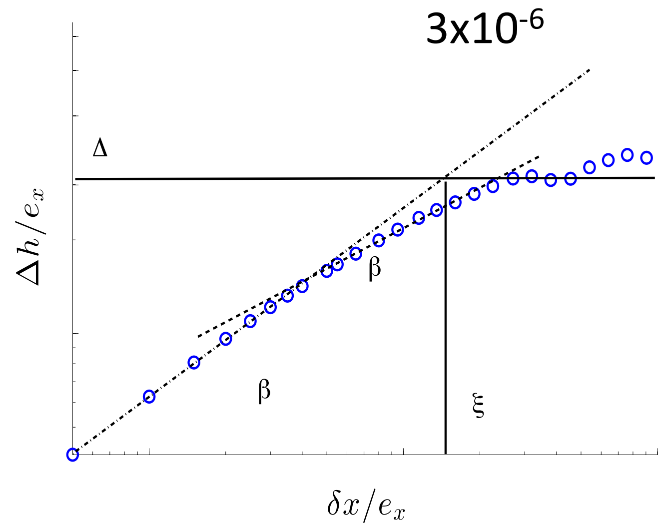

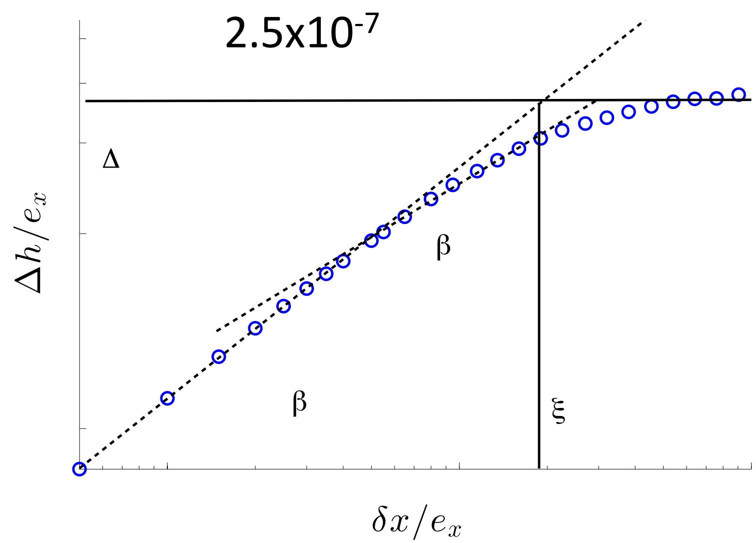

n=0.071, l_0/e_x=5.83

- Transition from persistent to anti-persistent (at about $4e_x$) to a smooth surface at 14-15e_x at the lower rates and 19e_x at the high rate.
- The transition lengths are relatively independent of rate until the higher rates.

UNT
UNIVERSITY OF NORTH TEXAS

Revisiting the Scaling of the Correlation Function

β=0.61

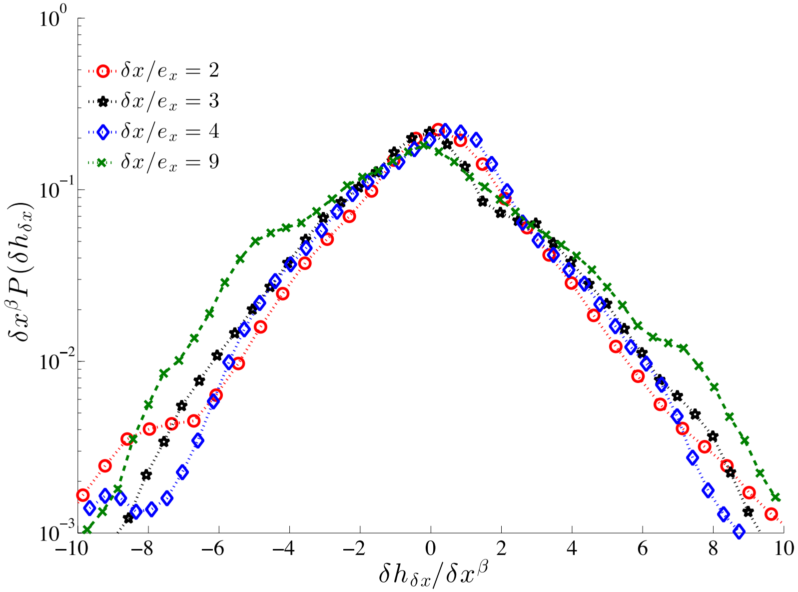

β=0.43

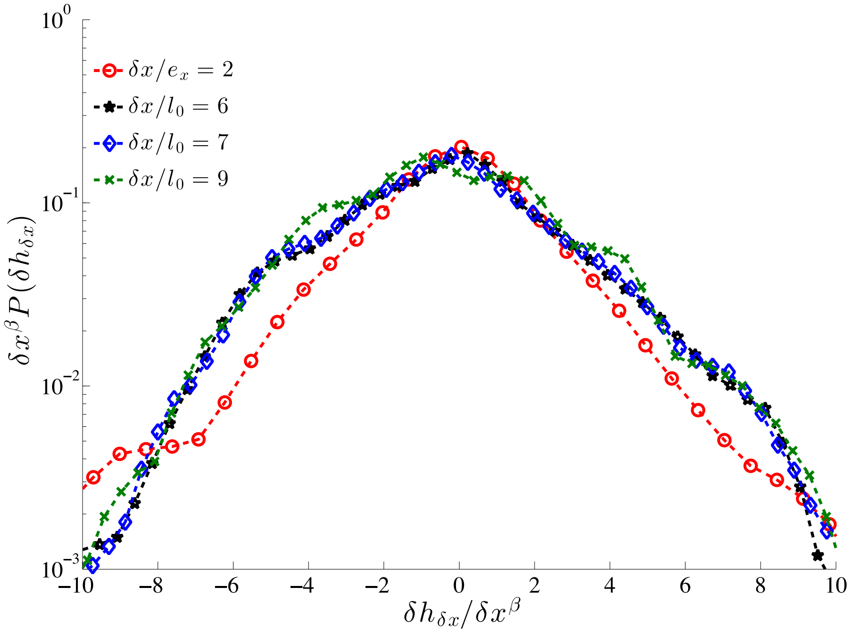

n=0.071, l_0/e_x=5.83

3×10^{-6}

UNIVERSITY OF NORTH TEXAS

Revisiting the Scaling of the Correlation Function

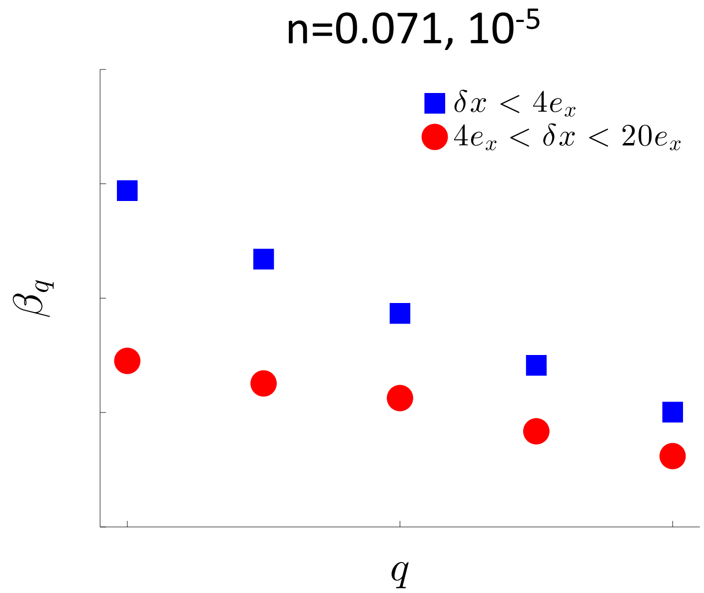

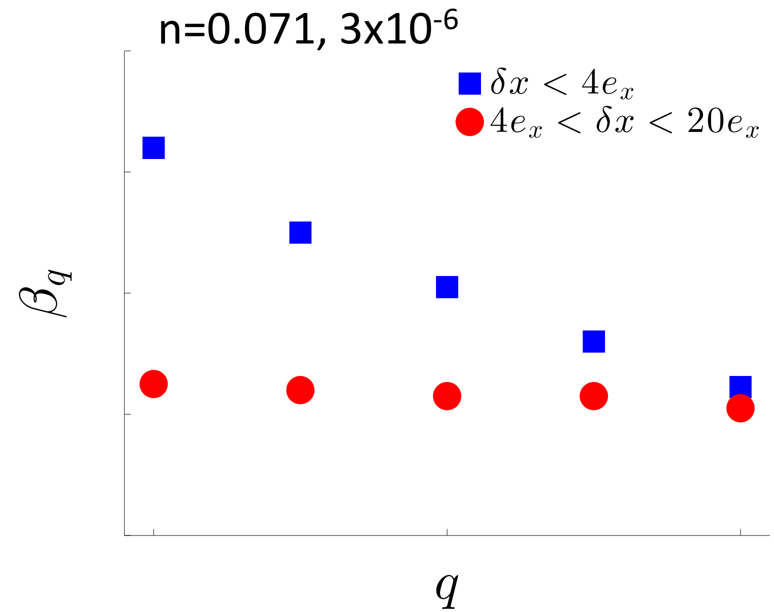

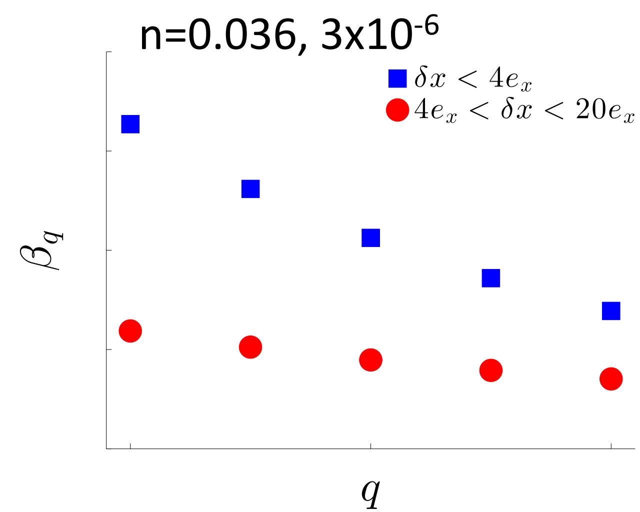

$$\Delta h_q = \langle [h(x+\delta x, z) - h(x,z)]^q \rangle_{x,z}^{1/q} \sim \delta x^{\beta_q}$$

UNT
UNIVERSITY OF NORTH TEXAS

Revisiting the Scaling of the Correlation Function

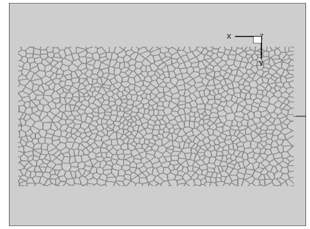

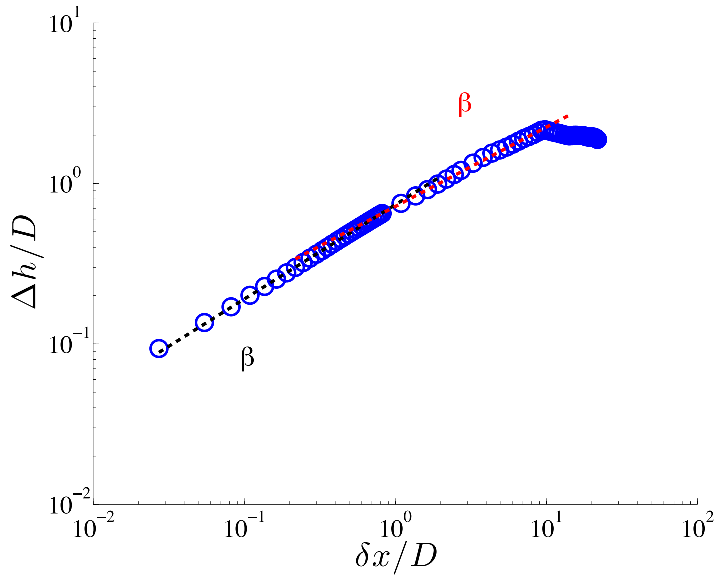

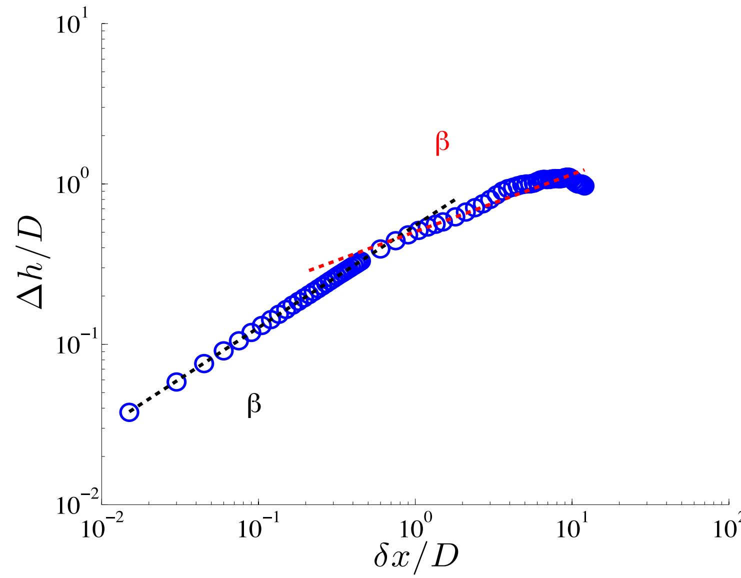

- Three regimes: (i) δx smaller than the mean grain size (β>0.5); (ii) δx larger than the mean grain size (β<0.5); (iii) straight crack. The small δx β is a fit from e_x to D/2, larger δx β is a fit from D to 2D.

UNIVERSITY OF NORTH TEXAS

Osovksi et al., Acta Mat., 82, 167, 2015.

Going Beyond the Correlation Function

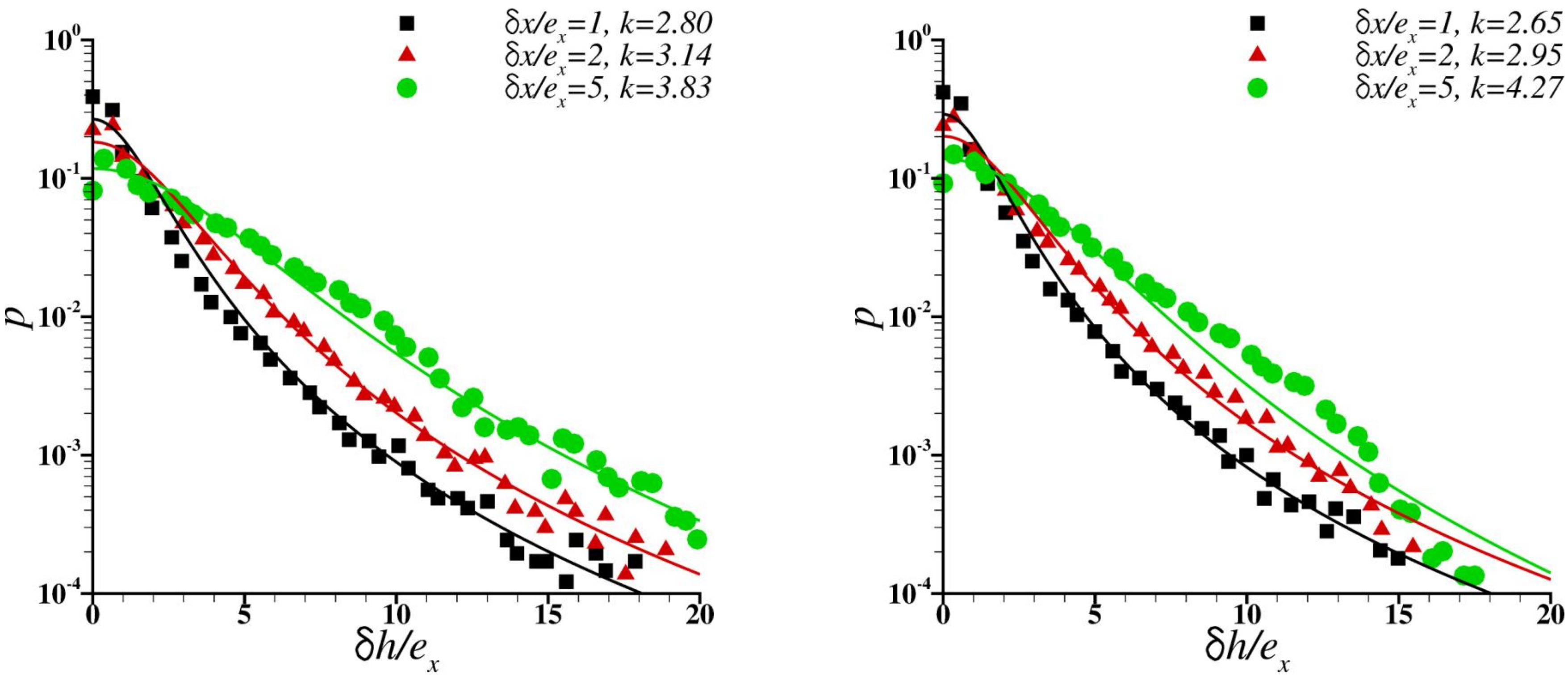

n=0.024 n=0.143

- Ductile fracture histograms have fat tails.
- Characterization via Student's t-distribution.
  - k going to infinity is the Gaussian limit.

$$p_{k,\delta h_c}(\delta h) \propto \frac{1}{\delta h_c}\left(1 + \frac{1}{k}\left(\frac{\delta h}{\delta h_c}\right)^2\right)^{-(k+1)/2}$$

UNT UNIVERSITY OF NORTH TEXAS

Going Beyond the Correlation Function

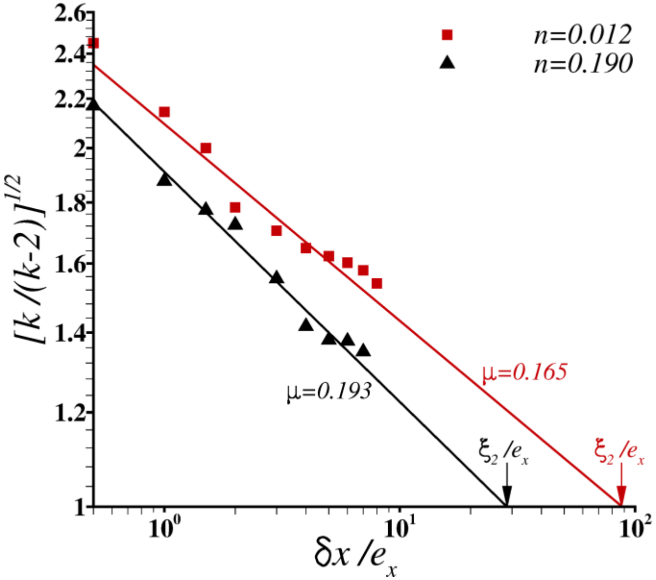

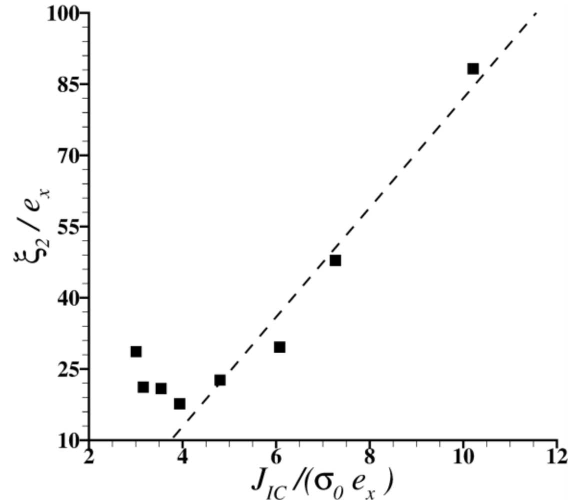

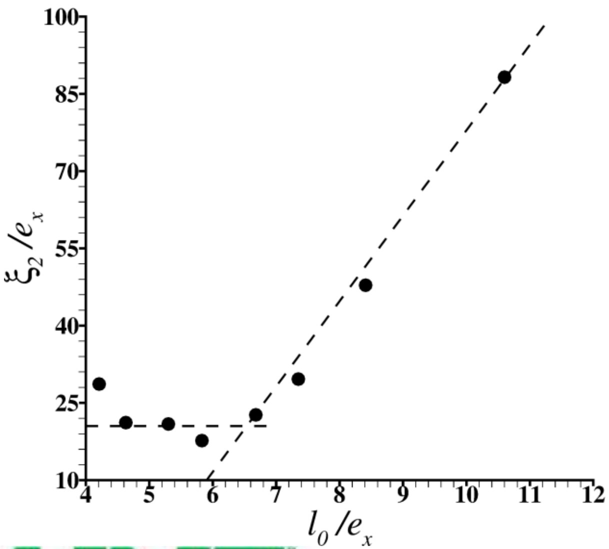

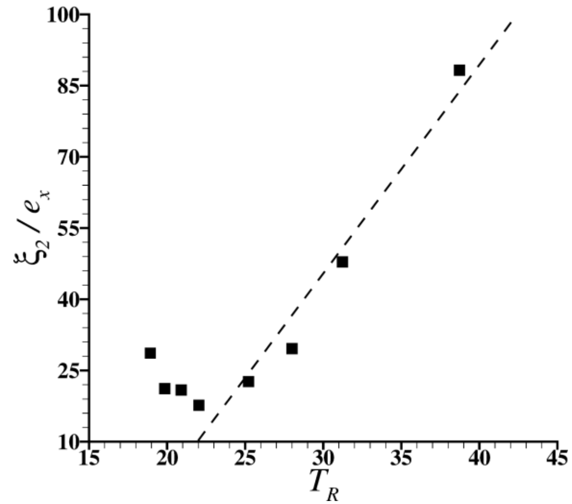

UNIVERSITY OF NORTH TEXAS

$$p_{k,\delta h_c}(\delta h) \propto \frac{1}{\delta h_c}\left(1+\frac{1}{k}\left(\frac{\delta h}{\delta h_c}\right)^2\right)^{-(k+1)/2}$$

Going Beyond the Correlation Function

- For the variation with rate, explored the use of the α-stable distributions S(α,β,σ,μ).
  - α is in the range between 0 and 2; 2 corresponds to a Gaussian distribution

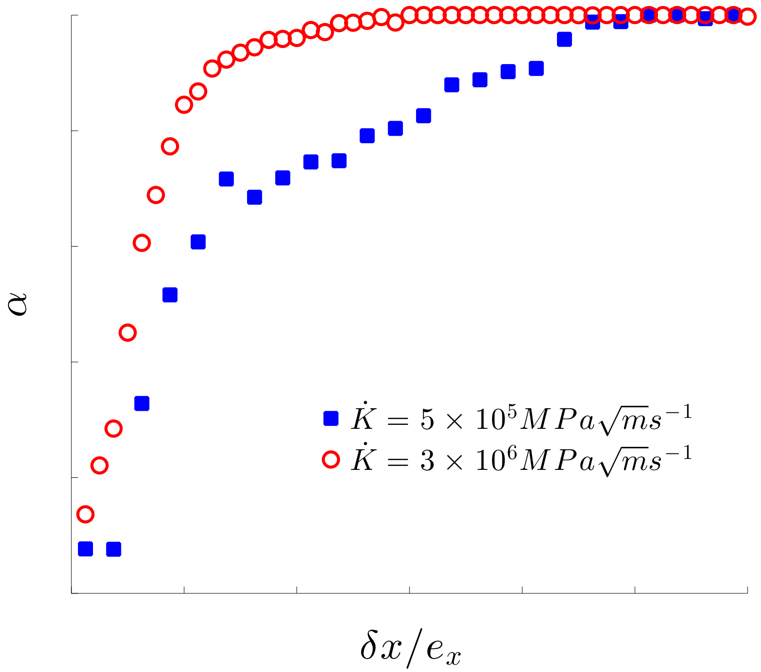

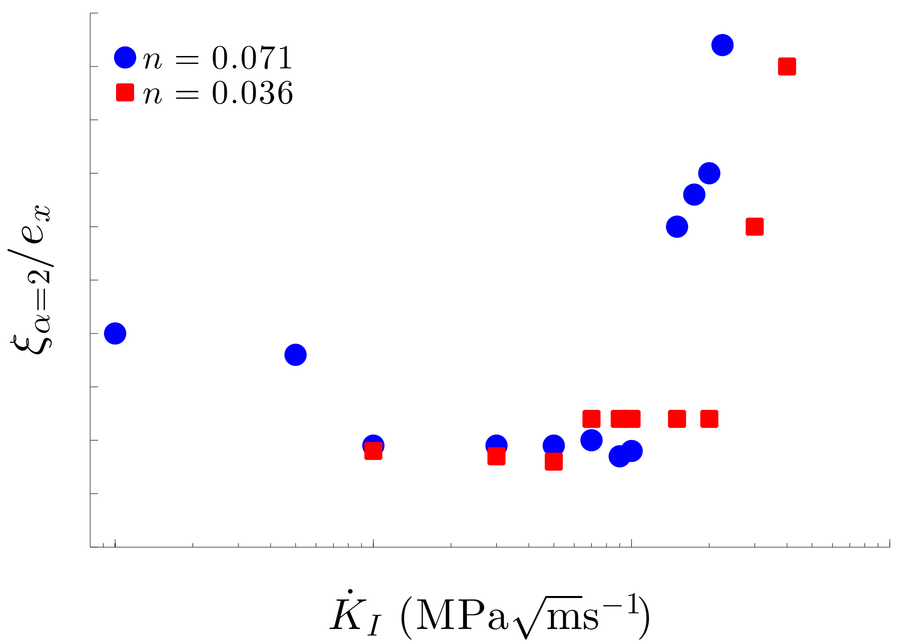

The correlation between $\xi_{\alpha=2}$ and J_{IC} and T_R was not as good as for Δh_s.

UNT
UNIVERSITY OF NORTH TEXAS

Crack Growth Along Grain Boundaries

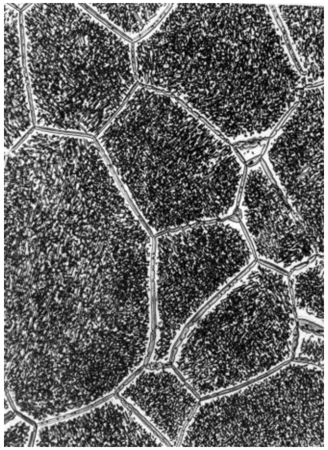

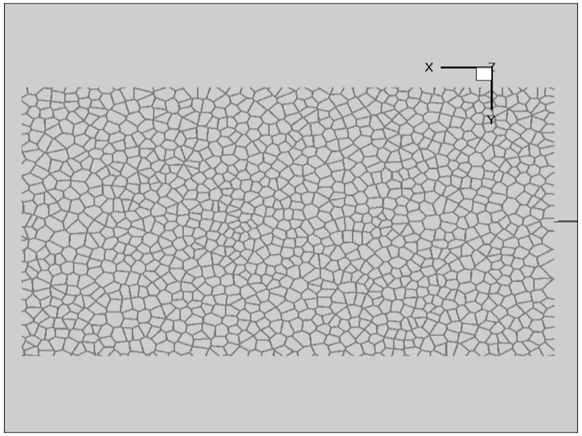

- The use of some of the most attractive lightweight metals is limited because they lack toughness due to room temperature grain boundary fracture, e.g. Al-Li alloys and meta-stable Ti β alloys.
- Modeled the effects of properties and microstructure on crack growth in meta-stable Ti β alloys.
  - Voronoi diagrams are used to generate a grain microstructure with mean grain size D.
  - One element thickness so the microstructure is 2D.
  - 1 cm fine mesh region ahead of the initial crack.

UNT UNIVERSITY OF NORTH TEXAS

Osovksi et al., Acta Mat., 82, 167, 2015.
Osovski et al., work in progress.

Crack Growth Along Grain Boundaries

Various grain sizes.

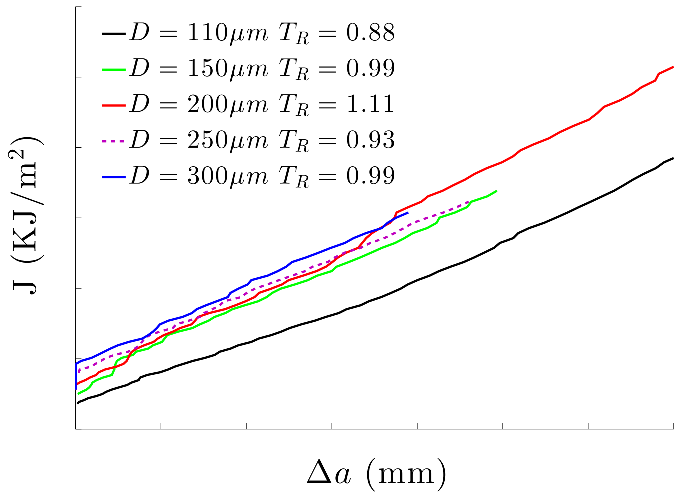

Fixed grain size, various realizations.

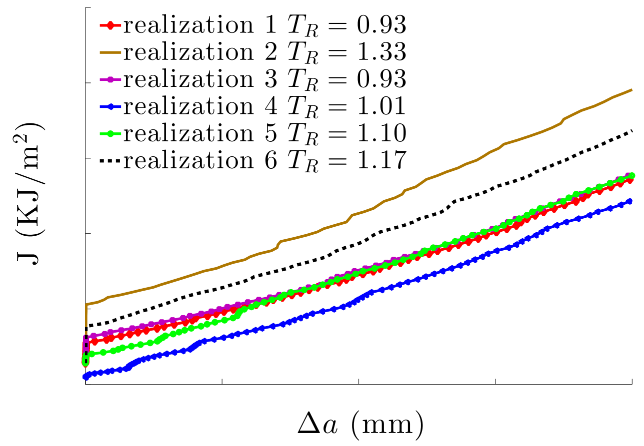

- 2D microstructure; 3D finite element formulation with 41,192,214 D.O.F.
- Grain boundary α layer thickness to mean grain size in the range 18 to 50.

Two realizations with the same mean grain size.

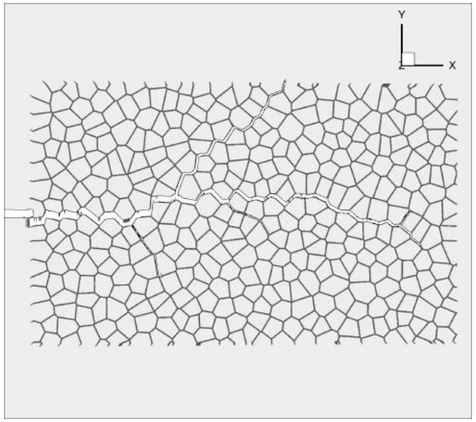

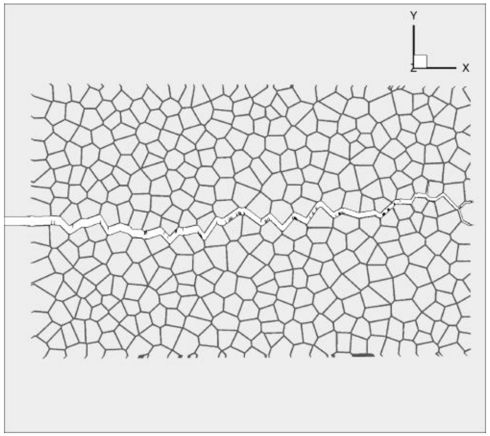

UNIVERSITY OF NORTH TEXAS

How Smart is a Crack?

Model prediction follows the actual path.

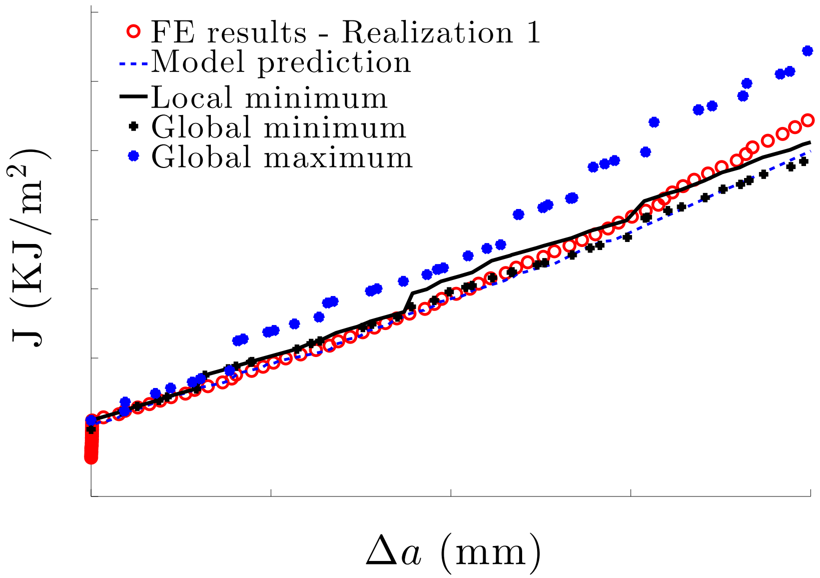

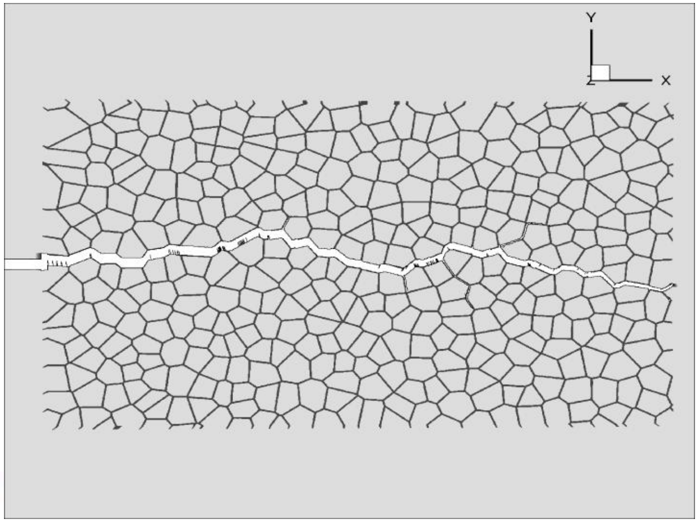

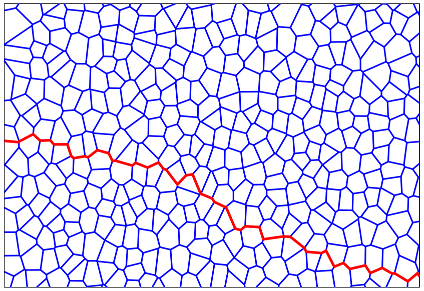

Global maximum

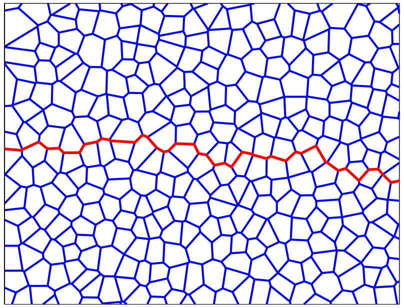

Local minimum

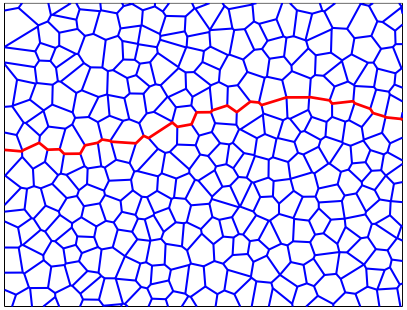

Global minimum

UNT
UNIVERSITY OF NORTH TEXAS

Concluding Remarks

- Can simulations such as these be used to design more fracture resistant material microstructures?
- Can parameters characterizing the fracture surface roughness be quantitatively related to parameters characterizing the material's crack growth resistance?
  - Results so far suggest that this can be done for void-by-void dominated ductile crack growth.
  - Is there a parameter (or a set of parameters) that can provide a quantitative toughness/roughness relation spanning the range from void-by-void dominated crack growth through multiple void interactions to distributed damage?
- Can parameters measuring the fracture surface provide a signature for identifying the mechanism of crack growth; for example identify a ductile-brittle transition?
- Needs: improved and more microscale fracture theories and improved computational capability.

UNT
UNIVERSITY OF NORTH TEXAS